Pediatric Radiology
https://doi.org/10.1007/s00247-020-04716-y

PICTORIAL ESSAY

Intracranial calcifications in childhood: Part 2

Fabricio Guimarães Gonçalves[1] · Luca Caschera[2] · Sara Reis Teixeira[1] · Angela Nicole Viaene[3] · Lorenzo Pinelli[4] · Kshitij Mankad[5] · César Augusto Pinheiro Ferreira Alves[1] · Xilma Rosa Ortiz-Gonzalez[6,7] · Savvas Andronikou[1,8] · Arastoo Vossough[1,8]

Received: 10 February 2020 / Revised: 3 April 2020 / Accepted: 12 May 2020

Abstract

This article is the second of a two-part series on intracranial calcification in childhood. In Part 1, the authors discussed the main differences between physiological and pathological intracranial calcification. They also outlined histological intracranial calcification characteristics and how these can be detected across different neuroimaging modalities. Part 1 emphasized the importance of age at presentation and intracranial calcification location and proposed a comprehensive neuroimaging approach toward the differential diagnosis of the causes of intracranial calcification. Pathological intracranial calcification can be divided into infectious, congenital, endocrine/metabolic, vascular, and neoplastic. In Part 2, the chief focus is on discussing endocrine/metabolic, vascular, and neoplastic intracranial calcification etiologies of intracranial calcification. Endocrine/metabolic diseases causing intracranial calcification are mainly from parathyroid and thyroid dysfunction and inborn errors of metabolism, such as mitochondrial disorders (MELAS, or mitochondrial myopathy, encephalopathy, lactic acidosis, and stroke-like episodes; Kearns–Sayre; and Cockayne syndromes), interferonopathies (Aicardi–Goutières syndrome), and lysosomal disorders (Krabbe disease). Specific noninfectious causes of intracranial calcification that mimic TORCH (toxoplasmosis, other [syphilis, varicella-zoster, parvovirus B19], rubella, cytomegalovirus, and herpes) infections are known as pseudo-TORCH. Cavernous malformations, arteriovenous malformations, arteriovenous fistulas, and chronic venous hypertension are also known causes of intracranial calcification. Other vascular-related causes of intracranial calcification include early atherosclerosis presentation (children with risk factors such as hyperhomocysteinemia, familial hypercholesterolemia, and others), healed hematoma, radiotherapy treatment, old infarct, and disorders of the microvasculature such as *COL4A1*- and *COL4A2*-related diseases. Intracranial calcification is also seen in several pediatric brain tumors. Clinical and familial information such as age at presentation, maternal exposure to teratogens including viruses, and association with chromosomal abnormalities, pathogenic genes, and postnatal infections facilitates narrowing the differential diagnosis of the multiple causes of intracranial calcification.

Keywords Brain · Calcification · Children · Computed tomography · Endocrine · Intracranial · Magnetic resonance imaging · Metabolic · Neoplastic · Physiological · Vascular

CME activity This article has been selected as the CME activity for the current month. Please visit the SPR website at www.pedrad.org on the Education page and follow the instructions to complete this CME activity.

✉ Fabricio Guimarães Gonçalves
goncalves.neuroradio@gmail.com

[1] Division of Neuroradiology, Department of Radiology, Children's Hospital of Philadelphia, 3401 Civic Center Blvd., Philadelphia, PA 19104, USA

[2] Neuroradiology Unit, Fondazione IRCCS Ca' Granda Ospedale Maggiore Policlinico, Milan, Italy

[3] Department of Pathology and Laboratory Medicine, Children's Hospital of Philadelphia, University of Pennsylvania Perelman School of Medicine, Philadelphia, PA, USA

[4] Neuroradiology Unit, Pediatric Neuroradiology Section, ASST Spedali Civili, Brescia, Italy

[5] Department of Radiology, Great Ormond Street Hospital, London, UK

[6] Division of Neurology, Department of Pediatrics, Children's Hospital of Philadelphia, Philadelphia, PA, USA

[7] Department of Neurology, University of Pennsylvania Perelman School of Medicine, Philadelphia, PA, USA

[8] Department of Radiology, University of Pennsylvania Perelman School of Medicine, Philadelphia, PA, USA

Published online: 08 July 2020

Introduction

This article is the second of a two-part series reviewing the imaging of intracranial calcification in childhood. In Part 1, we reviewed the histological features and how intracranial calcification is depicted across different neuroimaging modalities. We discussed the main differences between physiological and pathological intracranial calcification, emphasizing the relevance of age at presentation and intracranial calcification location. Moreover, we presented a comprehensive approach toward the differential diagnosis. Finally, we discussed congenital and infectious causes of intracranial calcification. In Part 2, we briefly review endocrine/metabolic, vascular, and neoplastic intracranial calcification etiologies.

Genetic causes of intracranial calcifications are extensive and manifest in different age groups during childhood. A comprehensive list of genetic entities that demonstrate intracranial calcification, and their respective Online Mendelian Inheritance in Man (OMIM) entries, affected genes, relevant clinical presentation, and key neuroimaging findings can be found in Table 1 [1–48].

Endocrine/metabolic causes of intracranial calcification

Endocrine/metabolic causes of intracranial calcification form a vast and heterogeneous group of diseases that sometimes mimic TORCH (toxoplasmosis, other [syphilis, varicella-zoster, parvovirus B19], rubella, cytomegalovirus and herpes) infections. Parathyroid and thyroid function abnormalities are well-known causes of intracranial calcification. During childhood, intracranial calcification secondary to hypothyroidism is less severe than in cases of parathyroid function abnormalities. In cases of hyper-, hypo-, and pseudohypoparathyroidism, the patterns of intracranial calcification, which are known to demonstrate metastatic calcification, are rather similar coursing with symmetrical basal ganglia, thalamic, and subcortical calcification [3].

Children with certain mitochondrial disorders and leukodystrophies might develop calcifications during the course of their disease. Another neurodegenerative disease associated with intracranial calcification is the idiopathic basal ganglia calcification-1 (IBGC1) or Fahr disease. Other causes include the channelopathies, such as *SCN3A* mutation (Fig. 1), which can also be associated with perisylvian polymicrogyria [49].

Parathyroid function abnormalities

Hyperparathyroidism

Hyperparathyroidism is defined by an abnormal parathyroid gland function, leading to elevated parathyroid hormone, and hypercalcemia. Hyperparathyroidism can be classified into primary, secondary, or tertiary. Primary hyperparathyroidism is usually caused by a parathyroid gland adenoma. Secondary hyperparathyroidism is related to an adaptive response to low serum levels of calcium or vitamin D, more commonly in chronic kidney disease. Tertiary hyperparathyroidism reflects a maladaptive response to antecedent hypocalcemia or vitamin D deficiency [50]. Intracranial calcification is very rare in hyperparathyroidism, more frequently described in adults [51]. It is even rarer in children, more frequently in pediatric chronic kidney disease, occurring in the cerebellum, dentate nucleus, caudate nucleus, putamen, thalamus, deep and periventricular white matter, and along the dura mater (Fig. 2) [52].

Hypoparathyroidism

Hypoparathyroidism is defined by an abnormal parathyroid gland function caused by a failure to produce the parathyroid hormone in response to hypocalcemia [53]. Hypoparathyroidism can be caused by congenital disorders and infiltration of the glands, or be iatrogenic [50]. Hypoparathyroidism is the most common potentially treatable cause of basal ganglia calcification [50]. Intracranial calcification is more common in the bilateral basal ganglia, particularly the globus pallidus [54, 55], and less common in the extrapyramidal system (Fig. 3) [44, 56].

Pseudohypoparathyroidism

Pseudohypoparathyroidism is a group of heterogeneous genetic disorders with end-organ resistance to parathyroid hormone (PTH) [57]. These children manifest with hypocalcemia, hyperphosphatemia, and increased serum concentration of PTH [57]. Pediatric pseudohypoparathyroidism is rare, and these children might show intracranial calcification more commonly in the basal ganglia, thalamus and subcortical white matter (Fig. 4) [58]. Several other diseases such as carbonic anhydrase deficiency might show a similar pattern of intracranial calcification as compared to hypoparathyroidism and pseudohypoparathyroidism, typically associated with osteopetrosis and renal tubular acidosis [28].

Thyroid function abnormalities

Hypothyroidism

Hypothyroidism is caused by an abnormal thyroid function associated with either low levels or absence of thyroid hormones. Hypothyroidism can be classified into congenital (present at birth) or acquired (later in life). Hypothyroidism can be further classified as primary, when the gland itself is affected, or secondary, where there are abnormalities in the hypothalamic–pituitary axis [59].

Table 1 Currently known genetic syndromes associated with intracranial calcification based on the OMIM database search engine

Entity	Gene	OMIM[a]	Clinical presentation	Neuroimaging findings
Neurocutaneous syndromes				
Tuberous sclerosis	*TSC1* *TSC2*	#191100 #613254	– Hamartomas in multiple organ systems (brain, skin, heart, kidneys and lung) – CNS manifestations include epilepsy, learning difficulties, behavioral problems and autism – Patients can also develop renal cysts and renal-cell carcinomas – Pulmonary lymphangioleiomyomatosis – Skin lesions (melanotic macules, facial angiofibromas and patches of connective tissue nevi)	– Cortical tubers – Cortical dysplasia – Subependymal nodules – Subependymal giant cell astrocytoma – *Calcification*: subependymal nodules, tubers, cortical dysplasia and retinal hamartomas
Sturge–Weber syndrome	*GNAQ*	#185300	– Multiple angiomas involving the face (typical port-wine stain) – Angiomas in the choroid of the eye, associated with glaucoma – Angiomas in the leptomeninges – Seizures – Mental retardation – Recurrent stroke-like episodes	– Prominent transmedullary veins – Enlarged choroid plexus – Leptomeningeal angiomatosis (leptomeningeal enhancement in the affected area) – Ipsilateral calvarial and regional sinus enlargement – *Calcification*: tram-track and gyriform
Basal cell nevus syndrome	*PTCH1* *PTCH2* *SUFU*	#109400	– Numerous basal cell cancers, epidermal cysts of the skin – Palmar and plantar pits – Calcified dural folds, keratocysts of the jaws – Ovarian fibromas, lymphomesenteric cysts – Medulloblastomas – Fetal rhabdomyomas – Bifid rib	– Multiple jaw keratocysts – Medulloblastoma in 5% – *Calcification*: dura mater
von Hippel–Lindau syndrome	*VHL*	#193300	– Angiomata of the retina – Hemangioblastoma of the cerebellum, brainstem, and spinal cord – Pheochromocytoma – Polycythemia	– CNS hemangioblastomas (cerebellum, brainstem, spinal cord) – *Calcification*: endolymphatic sac tumors
Mitochondrial disorders				
MELAS	*MTTL1* *MTTQ* *MTTH* *MTTK* *MTTC* *MTTS1* *MTND1* *MTND5* *MTND6* *MTTS2*	#540000	– Mitochondrial myopathy – Encephalopathy – Lactic acidosis – Stroke-like episodes – Seizures – Hemiparesis – Hemianopsia – Cortical blindness – Vomiting	– Stroke-like changes without a distinct vascular distribution, mostly cortical in the posterior and lateral brain – *Calcification*: scattered, punctate or faint in basal ganglia and thalamus
Kearns–Sayre syndrome	*MTTL2*	#530000	– Progressive external ophthalmoplegia – Ptosis – Pigmentary retinopathy – Cardiac conduction defects – Ataxia – Muscle weakness – Sensorineural hearing loss – Short stature – Dementia – Endocrine dysfunction – Elevated CSF protein	– T2-hyperintense lesions involving the subcortical U-fibers with sparing of the periventricular white matter, radially oriented T2 low signal stripes within the abnormal white matter – T2-hyperintense lesions in the bilateral globi pallidi with sparing of the putamina – Lesions in the dorsomedial thalamus and brainstem tegmental area – Brain atrophic changes are common neuroimaging manifestations – *Calcification*: basal ganglia and thalamus

Table 1 (continued)

Entity	Gene	OMIM[a]	Clinical presentation	Neuroimaging findings
Cockayne syndrome	*ERCC8* *ERCC6*	#216400 #133540	– Abnormal and slow growth and development within the first few years after birth – Cutaneous photosensitivity – Thin, dry hair – Progeroid appearance – Progressive pigmentary retinopathy – Sensorineural hearing loss – Dental caries – Disproportionately long limbs with large hands and feet	– Brain and cerebellar atrophy – White matter loss with slight parietal and occipital predominance – Lateral ventricular dilatation – *Calcification*: basal ganglia and cerebral cortex
Leukodystrophies associated with intracranial calcifications				
Aicardi–Goutières syndrome	*TREX1* *RNASEH2B* *RNASEH2C* *RNASEH2A* *SAMHD1* *ADAR* *IFIH1*	#225750	– Genetically heterogeneous encephalopathy – Cerebral atrophy – Leukodystrophy – Intracranial calcifications – Chronic CSF lymphocytosis – Increased CSF alpha-interferon – Negative serologic investigations for common prenatal infections – Similar to in utero viral infection – Progressive microcephaly – Spasticity – Dystonic posturing – Profound psychomotor retardation – Often death in early childhood	– Variable degree of frontotemporal white matter rarefaction – Cysts outside the frontotemporal regions – Variable intracranial calcification – *Calcification*: basal ganglia, cerebral white matter, thalamus, cerebellar hemispheres, dentate nucleus and brainstem
Krabbe disease	*GALC*	#245200	– Most patients present within the first 6 months of age with infantile or classic disease – Extreme irritability – Spasticity – Developmental delay – Severe motor and mental deterioration and death by age 2 years – Late onset in 10–15% of patients have a later onset	– Symmetrical cerebral and cerebellar demyelination – Changes in the basal nuclei and corpus callosum – Generalized brain atrophy with dilatation of the ventricles and subarachnoid spaces – ICC in the internal capsule and corona radiata – Thickening of the optic nerve/chiasm – *Calcification*: thalamus
Cystic leukoencephalopathy without megalencephaly	*RNASET2*	#612951	– Early-onset severe developmental delay – Microcephaly – Seizures – Hearing impairment – Clinically indistinguishable from congenital CMV infection	– Multifocal white matter hyperintensity – Anterior temporal cysts – Cortical malformation is uncommon – *Calcification*: radiologically indistinguishable from congenital CMV infection
Polycystic lipomembranous osteodysplasia with sclerosing leukoencephalopathy-1 (Nasu–Hakola disease)	*TYROBP*	#221770	– Presenile dementia – Large-scale destruction of cancellous bones – Initial symptoms starting in the 20s – Pain and swelling resulting from cysts in the wrists and ankles – Extremity bone fractures with minor trauma – Neuropsychiatric symptoms – Seizures – Agnosia – Apraxia	– Corpus callosum atrophy – Periventricular, basal ganglia and white matter calcification – Leukoencephalopathy – *Calcification*: basal ganglia and cerebellum [1, 2]
Leukoencephalopathy with calcification and cysts (Coats-plus disease)	*CTC1*	#612199	– Multisystem disorder – Retinal telangiectasia and exudates (Coats disease)	– Leukoencephalopathy (posterior gradient)

Table 1 (continued)

Entity	Gene	OMIM[a]	Clinical presentation	Neuroimaging findings
			– ICC with an associated leukoencephalopathy and brain cysts – Osteopenia with a tendency to fractures and poor bone healing – High risk of life-limiting gastrointestinal bleeding and portal hypertension	– Cysts (multiple, with mass effect and surrounding edema) – T2 hyperintensity in the periventricular, deep and sometimes subcortical white matter – *Calcification*: rock-like calcification in the basal ganglia, thalamus, dentate nucleus and deep cortex. Spot calcification within the deep white matter. Midbrain and pons may occur. Calcification within the walls of the cysts is common [3]
Leukoencephalopathy, brain calcifications, and cysts (Labrune syndrome)	*SNORD118*	#614561	– Seizures – Progressive neuro deficit – Intracranial hypertension – Headaches – Visual disturbance – Extrapyramidal, cerebellar and pyramidal features	– White matter changes – Cysts (cyst walls may calcify) – *Calcification*: extensive (basal ganglia, thalamus and dentate nucleus) [4, 5]
Cerebroretinal microangiopathy with calcifications and cysts-1	*CTC1*	#612199	– Retinal vascular abnormalities – Poor growth – Skeletal and hematological abnormalities – Recurrent gastrointestinal bleedings	– Leukoencephalopathy – Cysts [6] – *Calcification*: variable/extensive
Cerebroretinal microangiopathy with calcifications and cysts-2	*STN1*	#617341	– Premature aging – Pancytopenia – Hypocellular bone marrow – Osteopenia – Liver fibrosis – Vascular telangiectasia resulting in gastrointestinal bleeding	– Leukoencephalopathy – *Calcification*: variable [7]
Pseudo-TORCH syndromes				
Pseudo-TORCH syndrome-1 (band-like calcification with simplified gyration and polymicrogyria)	*OCLN*	#251290	– Clinical and neuroradiologic features that mimic intrauterine TORCH infection – Absence of evidence of infection – Congenital microcephaly – Intracranial calcifications – Severe developmental delay – Simplified gyration – Polymicrogyria – Severe developmental delay – Thrombocytopenia – Hepatic dysfunction – Hepatosplenomegaly	– Rudimentary pattern of brain development – Hour-glass appearance of the hemispheres and abnormal gyration (dysgyria) – Cerebellum, brainstem, and corpus callosum are typically hypoplastic – White matter volume is markedly reduced, with abnormally increased T2 signal and arrested myelination – *Calcification*: cortical bands, but also in the thalamus, cerebellum and pons [3]
Pseudo-TORCH syndrome-2	*USP18*	#607057	– Antenatal onset of intracranial hemorrhage – Microcephaly – Calcification – Brain malformations – Liver dysfunction – Thrombocytopenia – Respiratory insufficiency – Seizures – No evidence of an infectious agent	– Ventriculomegaly – Abnormal gyration of the temporal and parietal lobes – Pachygyria – Polymicrogyria – Gray matter heterotopia – Cerebellar hypoplasia – Cortical destruction – *Calcification*: periventricular and subcortical
Hemorrhagic destruction of the brain, subependymal calcification, and cataracts	*JAM3*	#613730	– Severe intrauterine destructive damage – Intracranial hemorrhage – Subependymal calcification	– *Calcification*: subependymal

Table 1 (continued)

Entity	Gene	OMIM[a]	Clinical presentation	Neuroimaging findings
			– Microcephaly – Congenital cataracts – Early death	
Idiopathic basal ganglia calcification				
Idiopathic basal ganglia calcification-1 (Fahr disease)	*SLC20A2*	#213600	– Symmetrical calcification in the basal ganglia and other brain regions – Patients may be asymptomatic or show a wide spectrum of symptoms – Extrapyramidal and psychiatric symptoms – Dystonia, poor balance and bradykinesia; seizures, developmental delay and progressive psychiatric symptoms such as aggressiveness and impulsivity – Serum levels of calcium, phosphate, alkaline phosphatase and parathyroid hormone are normal	– *Calcification*: basal ganglia (globus pallidus), thalamus, hippocampus, cerebral cortex, subcortical cerebral and cerebellar white matter and dentate nucleus
Small-vessel disease				
Brain small-vessel disease-1 with or without ocular anomalies	*COL4A1*	#175780	– Variable manifestations – Disruption of vascular basement membranes, particularly in the cerebral vasculature – Vessels are susceptible to hemorrhage – Clinical features thus reflect the location and severity of the vascular defect, including impaired neurologic development or function, hemiplegia, seizures and variable ocular anomalies	– Porencephaly – Hemosiderin deposition – Lacunar infarcts – Enlarged ventricles – Leukoencephalopathy – Schizencephaly – *Calcification*: adjacent brain changes [8]
Brain small-vessel disease-2	*COL4A2*	#614483	– Variable neurologic impairment – Disturbed vascular supply that leads to cerebral degeneration	– Porencephaly – Periventricular leukoencephalopathy – Cerebellar hypoplasia – Cerebral atrophy – *Calcification*: adjacent brain changes [9]
Other causes				
Familial focal epilepsy with variable foci-4	*SCN3A*	#617935	– Focal seizures in the first years of life – Mild cognitive impairment – Speech delay – Attention deficit-hyperactivity – Learning disabilities	– Subcortical flame-shaped marked hyperechogenicity – Undersulcation and underopercularization of the frontal and temporal lobes – Frontoparietal polymicrogyria/pachygyria – Diffuse white matter signal changes – *Calcification*: flame-shaped subcortical calcifications
Revesz syndrome	*TINF2*	#268130	– Bilateral exudative retinopathy – Severe aplastic anemia – Intrauterine growth retardation – Fine sparse hair – Fine reticulate skin pigmentation – Ataxia because of cerebellar hypoplasia	– *Calcification*: subcortical white matter, basal ganglia, thalamus and internal capsule [10]
Hyperphenylalaninemia (dihydropteridine reductase deficiency)	*QDPR*	#261630	– Hyperphenylalaninemia – Global developmental delay – Involuntary movements – Seizures	– *Calcification*: basal ganglia [11]
Spastic paraplegia-56	*CYP2U1*	#615030	– Spastic paraplegia (upper limbs)	– White matter lesions

Table 1 (continued)

Entity	Gene	OMIM[a]	Clinical presentation	Neuroimaging findings
			– Delayed walking – Toe walking – Unsteady gait – Spastic gait – Hyperreflexia of the lower limbs and extensor plantar responses	– Thin corpus callosum – *Calcification*: globus pallidus [12]
Cerebrotendinous xanthomatosis	*CYP27A1*	#213700	– Progressive neurologic dysfunction – Cerebellar ataxia beginning after puberty – Systemic spinal cord involvement and a pseudobulbar phase leading to death – Premature atherosclerosis and cataracts – Large deposits of cholesterol and cholestanol found in virtually every tissue, particularly the Achilles tendons, brain and lungs	– Supratentorial atrophy – Deep white matter changes – T2 hyperintensities (dentate nucleus, globus pallidus, substantia nigra and inferior olivary nucleus) – *Calcification*: dentate nucleus [13]
Oculodentodigital dysplasia	*GJA1*	#164200	– Constellation of neurologic manifestations – Bilateral microphthalmia – Abnormally small nose – Hypotrichosis – Dental anomalies – Fifth finger camptodactyly – Syndactyly of the fourth and fifth fingers – Missing toe phalanges	– White matter changes – *Calcification*: basal ganglia and dentate nucleus [14, 15]
Adams–Oliver syndrome-1	*ARHGAP31*	#100300	– Aplasia cutis congenita of the scalp vertex – Terminal transverse limb defects (e.g., amputations, syndactyly, brachydactyly or oligodactyly) – In addition, vascular anomalies such as cutis marmorata telangiectatica congenita, pulmonary hypertension, portal hypertension and retinal hypervascularization – Congenital heart defects	– Hypoplastic corpus callosum – Bilateral hemispheric corticosubcortical hemorrhagic lesions – Microcephaly – Pachygyria, polymicrogyria, dysplasia, heterotopia, schizencephaly and colpocephaly – Ischemia – Infarct – Periventricular leukomalacia – *Calcification*: periventricular [16]
Raine syndrome (osteosclerotic bone dysplasia)	*FAM20C*	#259775	– Microcephaly – Hypoplastic nose – Gum hyperplasia – Cleft palate – Low-set ears – Neonatal osteosclerotic bone dysplasia – Early and aggressive onset with death within the first few weeks after birth – Narrow prominent forehead, proptosis, depressed nasal bridge and midface hypoplasia	– Generalized increase in the density of all bones – Marked increase in the ossification of the skull – Increased ossification of the basal structures of the skull and facial bones – Periosteal bone formation – Sequelae of vascular dysfunction (ischemia, infarct, periventricular leukomalacia) – *Calcification*: adjacent the brain changes [16, 17]
Papillon–Lefèvre syndrome	*CTSC*	#245000	– Palmoplantar keratoderma – Periodontitis – Premature loss of dentition	– *Calcification*: dura mater [18]
Spondyloenchondrodysplasia with immune dysregulation	*ACP5*	#607944	– Spondyloenchondrodysplasia – Typical metaphyseal and vertebral bone lesions – Immune dysfunction – Neurologic involvement	– *Calcification*: basal ganglia and subcortical [19]

Table 1 (continued)

Entity	Gene	OMIM[a]	Clinical presentation	Neuroimaging findings
Molybdenum cofactor deficiency A	*MOCS1*	#252150	– Neonatal onset of intractable seizures – Opisthotonus – Facial dysmorphism – Hypouricemia – Elevated urinary sulfite levels – Severe neurologic damage – Death in early childhood	– Subcortical cystic changes – Parenchymal loss – White matter gliosis – Cerebral atrophy (enlargement of the ventricular and cortical sulci, interhemispheric fissure and thinning of the corpus callosum) [20] – *Calcification*: basal ganglia and thalamus
Sulfite oxidase deficiency	*SUOX*	#272300	– Fatal neurologic disease – Ectopia lentis – Increased sulfite in urine with markedly decreased inorganic sulfate excretion – Developmental delay – Ataxic gait – Dystonia – Choreoathetosis	– Acute: loss of gray–white matter differentiation and edema in the cerebral cortex and basal ganglia – Chronic: cystic encephalomalacia in the subcortical white matter, external capsules, basal ganglia, ventriculomegaly and diffuse cerebral atrophy, which may be consistent with ulegyria and thinning of the corpus callosum – *Calcification*: thalamus and basal ganglia [20, 21]
Fabry disease	*GLA*	#301500	– Systemic disease – Progressive renal failure – Cardiac disease – Cerebrovascular disease – Small-fiber peripheral neuropathy – Skin lesions	– Ischemic lesions (small vessels), especially of the posterior circulation – T2 hyperintensities in the white matter of the frontal and parietal lobes – T1 hyperintensity in the deep gray matter, especially that of the pulvinar, relating to mineralization – Exclusive involvement of pulvinar is thought to be characteristic – Basilar artery dolichoectasia is characteristic of this disease – Both T2 and T1 changes have been seen to regress with treatment if instituted early enough – *Calcification*: basal ganglia and thalamus (pulvinar) [22, 23]
Celiac disease, epilepsy with bilateral occipital calcifications		226810	– Celiac disease – Folate and iron deficiency – Epilepsy	– *Calcification:* parieto-occipital subcortical [24]
Rajab interstitial lung disease with brain calcifications	*FARSB*	#613658	– Developmental delay – Small stature – Retinopathy and microcephaly – Highly variable phenotype – Infancy or early childhood – Poor growth – Interstitial lung disease – Liver, skeletal and renal abnormalities	– *Calcification*: extensive scattered in the basal ganglia and cortex [25]
Diencephalic–mesencephalic junction dysplasia syndrome-1	*PCDH12*	#251280	– Progressive microcephaly – Severely delayed or even absent psychomotor development with profound intellectual disability – Spasticity or dystonia – Seizures and/or visual impairment	– Developmental malformation of the midbrain – *Calcification*: subcortical, basal ganglia and thalamus [26]
Carbonic anhydrase II (osteopetrosis)	*CA2*	#259730	– Renal tubular acidosis – Osteopetrosis – Brain calcifications – Developmental delay	– Brain calcification generally progressive

Table 1 (continued)

Entity	Gene	OMIM[a]	Clinical presentation	Neuroimaging findings
			– Short stature – Craniofacial disproportion with large cranial vault and broad forehead – Strabismus – Nystagmus	– Basal ganglia, thalami and gray–white matter junction in frontal regions more than posterior regions – Intracranial calcification similar to that seen in hypoparathyroidism and pseudohypoparathyroidism [27, 28]
Generalized arterial calcification of infancy-1 and infancy-2	*ENPP1* *ABCC6*	#208000 #614473	– Calcification of the internal elastic lamina of muscular arteries – Arterial stenosis from myointimal proliferation – Often fatal within the first 6 months of age because of myocardial ischemia resulting in refractory heart failure	– *Calcification*: vascular
Brain abnormalities, neurodegeneration and dysosteosclerosis	*CSF1R*	#618476	– Brain abnormalities – Progressive neurologic deterioration – Sclerotic bone dysplasia similar to dysosteosclerosis – Age at onset is highly variable – Hydrocephalus – Global developmental delay – Hypotonia	– Periventricular white matter abnormalities – Large cisterna magna or Dandy–Walker malformation – Agenesis of the corpus callosum – *Calcification*: periventricular [29]
Phenylketonuria	*PAH*	#261600	– Mental retardation – Mouse-like odor – Light pigmentation – Gait, stance and sitting posture abnormalities – Eczema – Epilepsy	– *Calcification*: white matter [30]
Keutel syndrome	*MGP*	#245150	– Multiple peripheral pulmonary stenosis – Sensorineural hearing loss – Short terminal phalanges – Calcification and ossification of the cartilage in the external ears, nose, larynx, trachea and ribs	– Calcifications of the cartilage of the pinna – Stenosis or occlusion of the terminal segments of the major intracranial arteries – Collateral moyamoya vessels seen at skull base or in basal ganglia – Hyperintense signal abnormalities of the subcortical and periventricular white matter on T2-weighted and FLAIR imaging – Chronic ischemic changes – Focal encephalomalacic changes – *Calcification*: isolated foci in the cortical–subcortical white matter [31]
Primrose syndrome	*ZBTB20*	#259050	– Recognizable facial features – Macrocephaly – Intellectual disability – Enlarged and calcified external ears (pina) – Sparse body hair and distal muscle wasting – Sensorineural hearing loss – Hypotonia – Cryptorchidism – Macrocephaly	– Corpus callosum dysgenesis – *Calcification*: basal ganglia [32, 33]
Early infantile epileptic encephalopathy-49	*DENND5A*	#617281	– Microcephaly – Seizures in the neonatal period – Global developmental delay – Intellectual disability – Lack of speech	– Enlarged ventricles – Dysgenesis of the corpus callosum – Dandy–Walker malformation – Hypoplastic vermis – Hydrocephalus [34]

Table 1 (continued)

Entity	Gene	OMIM[a]	Clinical presentation	Neuroimaging findings
			– Hypotonia – Spasticity – Coarse facial features	– *Calcification*: basal ganglia and periventricular
Biotinidase deficiency	*BTD*	#253260	– Axia – Alopecia – Skin rash	– *Calcification*: basal ganglia [35]
Folate malabsorption	*SLC46A1*	#229050	– Folate deficiency within a few months after birth – Low blood and cerebrospinal fluid folate levels with megaloblastic anemia – Diarrhea – Immune deficiency – Infections – Neurologic deficits	– *Calcification*: basal ganglia, thalamus and generalized [36]
Brachyolmia Type 2		#613678	– Bone dysplasia – Short trunk dwarfism – Platyspondyly – No significant long-bone abnormalities	– *Calcification*: falx [37]
Marshall syndrome	*COL11A1*	#154780	– Midfacial hypoplasia – Cleft palate – Ocular anomalies (high myopia and cataracts) – Sensorineural hearing loss – Short stature with spondyloepiphyseal dysplasia and arthropathy	– Hypoplasia of the maxilla, nasal bones and frontal sinuses – Calvarial thickening – Narrowed joint spaces, with osteophytic degeneration in the hips and knees – *Calcification*: falx cerebri and meninges [38]
Proteasome-associated auto-inflammatory syndrome	*PSMB8*	#256040	– Early childhood onset – Annular erythematous plaques on the face and extremities – Partial lipodystrophy – Immune dysregulation – Recurrent fever – Severe joint contractures – Muscle weakness – Atrophy – Hepatosplenomegaly	– *Calcification*: basal ganglia [39]
Xeroderma pigmentosum, Group B	*ERCC3*	#610651	– Thin, dry skin showing wrinkling, checkered pigmentation, small dilatations of the vessels, skin contraction and development of skin-based tumors – Neurologic abnormalities – Dwarfism, gonadal hypoplasia and mental deficiency	– Cerebral atrophy – Ventricular dilation – *Calcification*: basal ganglia and cerebral cortex [40]
Pseudohypoparathyroidism Type IA	*GNAS*	#103580	– PTH resistance – Short stature – Obesity – Round facies – Subcutaneous ossifications – Brachydactyly – Skeletal anomalies – Some patients have mental retardation	– *Calcification*: basal ganglia, thalamus and deep gyral [3]
Dentatorubral-pallidoluysian atrophy (Haw River syndrome)	*ATN1*	#125370	– Progressive ataxia – Myoclonus – Epilepsy – Choreoathetosis – Dystonia	– Cerebellar, tegmental and cerebral atrophy – White matter signal changes – Signal changes in the pons, midbrain, thalamus and globus pallidus

Table 1 (continued)

Entity	Gene	OMIM[a]	Clinical presentation	Neuroimaging findings
			– Dementia – Psychiatric symptoms – Intellectual disability	– *Calcification*: basal ganglia
Kenny–Caffey syndrome, Type 2	*FAM111A*	#127000	– Short stature – Cortical thickening and medullary stenosis of the tubular bones – Delayed closure of the anterior fontanel – Eye abnormalities – Transient hypocalcemia	– *Calcification*: basal ganglia, dentate nuclei and cerebellum [41]
Fibrodysplasia ossificans progressiva	*ACVR1*	#135100	– Progressive ossification of skeletal muscle, fascia, tendons and ligaments – Individuals appear normal at birth – Great toes are short, deviated and monophalangic – Limited neck movement	– Transient dentate nuclei signal changes – Tissue proliferation surrounding the brainstem – Brainstem hamartomatous lesions and dysmorphisms [42, 43] – *Calcification*: basal ganglia and/or dentate nucleus
Familial isolated hypoparathyroidism-1 and -2	*PTH* *GCM2*	#146200 #618883	– Hypoparathyroidism – Hypocalcemia	– *Calcification*: basal ganglia, thalamus and subcortical white matter [44]
Hypoparathyroidism, sensorineural deafness and renal disease (Barakat syndrome)	*GATA3*	#146255	– Hypoparathyroidism – Hypocalcemia – Deafness – Renal dysplasia	– *Calcification*: basal ganglia, thalamus and subcortical white matter [45]
Hypocalcemia, autosomal dominant-1	*CASR*	#601198	– Hypoparathyroidism – Hypocalcemia	– *Calcification*: basal ganglia [46]
Hypocalcemia, autosomal dominant-2	*GNA11*	#615361	– Hypocalcemia – Parathyroid hormone in the low–normal range	– *Calcification*: basal ganglia, thalamus, subcortical and dentate nucleus [47]
X-linked mental retardation syndrome (Fried syndrome/Pettigrew syndrome)	*AP1S2*	#304340	– Mental retardation – Choreoathetosis – Seizures – Iron or calcium deposition in the brain	– Hydrocephalus – Dandy–Walker type malformation – *Calcification*: basal ganglia [48]

CNS central nervous system, *CMV* cytomegalovirus, *CSF* cerebrospinal fluid, *ICC* intracranial calcification, *FLAIR* fluid-attenuated inversion recovery, *MELAS* mitochondrial myopathy, encephalopathy, lactic acidosis and stroke-like episodes, *PTH* parathyroid hormone, *TORCH* toxoplasmosis, other [syphilis, varicella-zoster, parvovirus B19], rubella, cytomegalovirus and herpes

[a] OMIM: Online Mendelian Inheritance in Man (https://www.ncbi.nlm.nih.gov/omim)

Intracranial calcification is more frequent in cases of congenital hypothyroidism. In these cases, intracranial calcification is typically located in the bilateral basal ganglia and subcortical white matter (Fig. 5) [60].

Mitochondrial disorders

Primary mitochondrial disorders such as MELAS (mitochondrial myopathy, encephalopathy, lactic acidosis and stroke-like episodes) and Kearns–Sayre syndrome are known causes of intracranial calcifications. Other disorders with secondary mitochondrial dysfunction, such as Cockayne syndrome, also might exhibit intracranial calcification.

Mitochondrial myopathy, encephalopathy, lactic acidosis and stroke-like episodes

MELAS (OMIM #540000) is one of the most common primary mitochondrial disorders. The most common clinical features include stroke-like episodes before the fourth decade, lactic acidemia, muscle weakness, recurrent headaches, hearing impairment, short stature and cortical vision loss [61]. Typical neuroimaging findings include stroke-like migrating brain changes, often without a distinct vascular distribution (mostly cortical in the posterior and lateral brain), bilateral symmetrical abnormalities in the deep gray matter and brainstem and diffuse white matter signal changes along with brain and cerebellar atrophy. Magnetic resonance spectroscopy might show a decrease in the *N*-acetylaspartate (NAA)

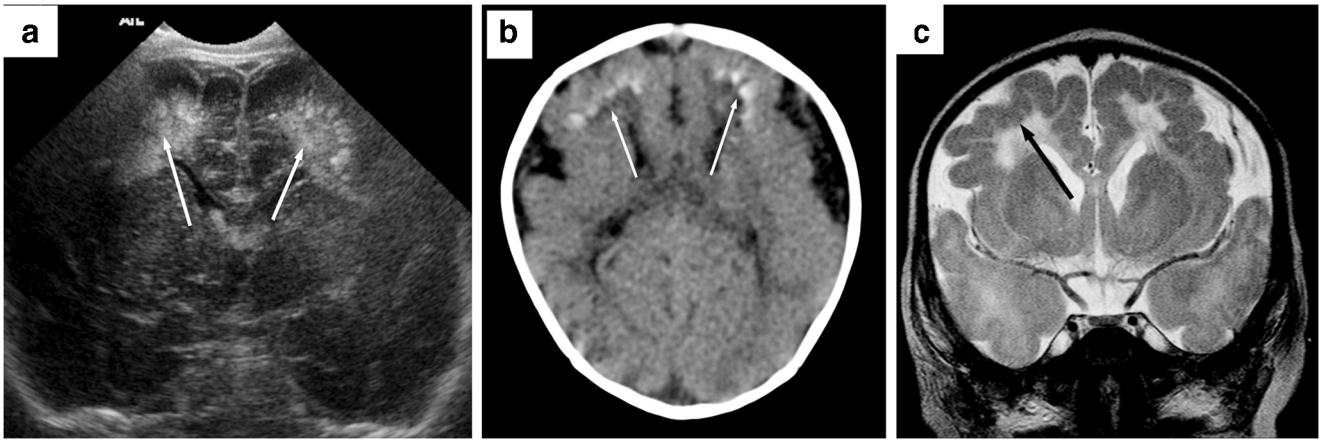

Fig. 1 Sodium channelopathy *SCN3A* in a 2-month-old boy with apnea and seizures. **a** Coronal neurosonography image shows the subcortical flame-shaped marked hyperechogenicity in both frontal lobes (*arrows*). **b** Axial CT image shows the abnormal appearance of the brain, with thickened cortex bilaterally, undersulcation and underopercularization of the frontal and temporal lobes. Note again the flame-shaped calcifications at the gray–white junction in the bilateral frontal lobes (*arrows*). **c** Coronal T2-weighted MRI shows a pattern of extensive bilateral symmetrical, predominantly frontoparietal, polymicrogyria/pachygyria (*arrow*) and diffuse white matter signal changes

peak and an increase in the lactate peak. Scattered, punctate or faint calcifications might be found in the bilateral thalami and basal ganglia on CT or MRI, particularly as children get older (Fig. 6) [62].

Kearns–Sayre syndrome

Kearns–Sayre syndrome (OMIM #530000) is a rare primary mitochondrial disorder. The main clinical findings include progressive external ophthalmoplegia, ptosis, pigmentary retinopathy, cardiac conduction defects, ataxia, muscle weakness, sensorineural hearing loss, short stature, dementia, endocrine dysfunction and elevated cerebrospinal fluid (CSF) proteins with onset age before 20 years [63]. Neuroimaging findings range from unremarkable to severe. Common neuroimaging manifestations on MRI include T2-hyperintense lesions involving the subcortical U-fibers with sparing of the periventricular white matter, radially oriented T2-W low signal stripes within the abnormal white matter, T2-hyperintense lesions in the bilateral globi pallidi with sparing of the putamina and lesions in the dorsomedial thalamus and brainstem tegmentum, along with brain atrophic changes. Calcification might be seen in the basal ganglia (globi pallidi and caudate nuclei) in the late stages of the disease (Fig. 7) [64].

Cockayne syndrome

Cockayne syndrome (OMIM CSA #216400/CSB #133540) is a rare entity that manifests as accelerated aging and cachectic dwarfism [65]. Other features include microcephaly, dysmorphic facies, failure to thrive, developmental delay, photosensitivity, sensorineural hearing loss and early cataracts [66].

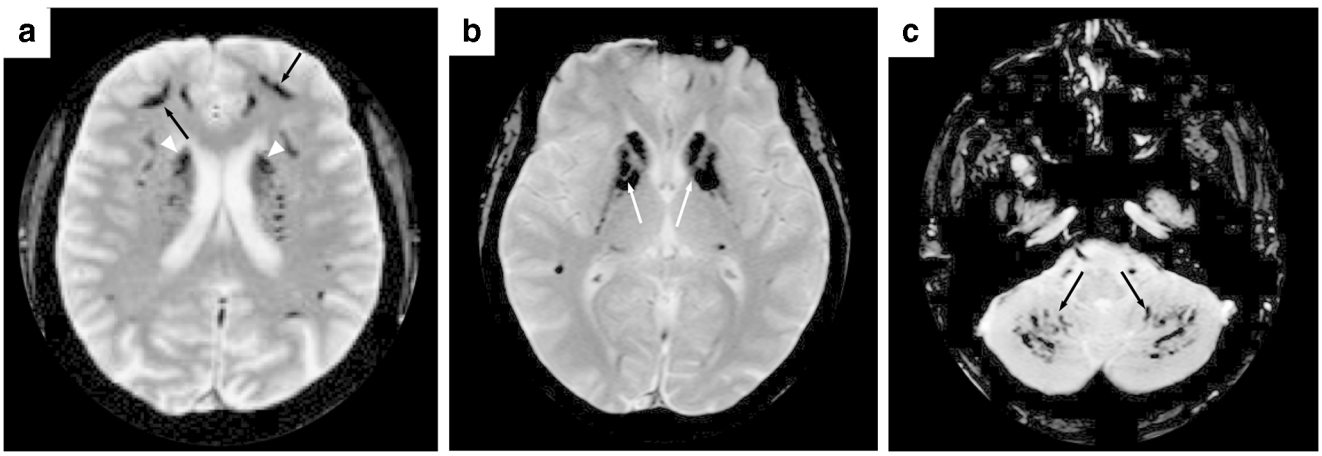

Fig. 2 Hyperparathyroidism from chronic kidney disease in a 14-year-old boy. **a**–**c** Axial T2*-weighted MRI (**a**) shows bilateral and symmetrical caudate nuclei (*arrowheads*) and subcortical calcification (*arrows*). In (**b**), note the coarse bilateral and symmetrical basal ganglia (caudate and putamen) calcification (*arrows*). Symmetrical and bilateral cerebellar calcification is demonstrated in (**c**) (*arrows*)

Fig. 3 Hypoparathyroidism in a 5-year-old girl with a history of short stature and pituitary dwarfism. She was scanned because of headache, hypertension, and vomiting. Axial nonenhanced CT shows bilateral coarse and extensive calcification in the bilateral putamina (*arrows*) and bilateral punctate deep and subcortical white matter calcification in the frontal lobes (*arrowheads*)

Recent publications have found that mitochondrial dysfunction might contribute to the pathophysiology of this disorder [65]. Neuroimaging findings include brain and cerebellar atrophy (from mild to severe), white matter loss with slight parietal and occipital predominance, lateral ventricular dilatation, reduced choline-to-creatine (Cho/Cr) ratios in the white matter and intracranial calcification. Bilateral and symmetrical basal ganglia calcifications, ranging from punctate to severe, mostly located in the putamina, are frequently seen. Calcifications have also been reported in the cerebral cortex at the depth of the sulci, in the dentate nucleus, in the basal ganglia (caudate and globi pallidi), in the thalami and along the leptomeningeal vessels (Fig. 8) [67, 68].

Fig. 4 Pseudohypoparathyroidism in a 13-year-old boy with a history of autism scanned because of headache. Axial nonenhanced CT image shows symmetrical arc-like subcortical calcifications predominantly involving the frontal lobes, bilaterally (*arrowheads*). Calcifications are also seen in the bilateral putamen and globus pallidus (*arrows*)

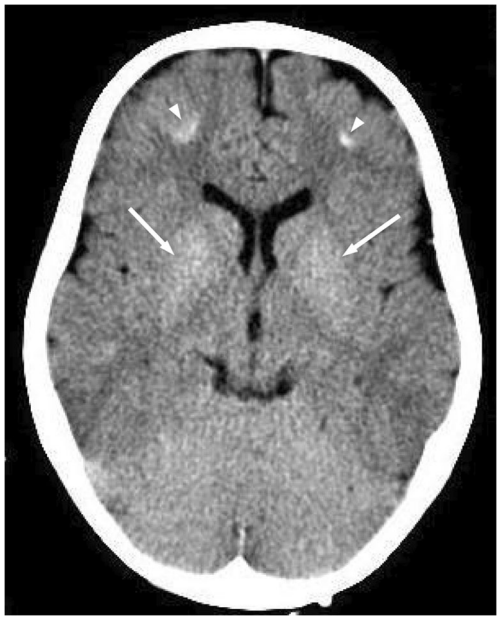

Fig. 5 Subclinical hypothyroidism in a 2-year-old boy. Axial nonenhanced CT was performed because of somnolence and hyporeactivity following head trauma. Note the fine subcortical calcification in the frontal lobes (*arrowheads*) and the bilateral putamina (*arrows*)

Pseudo-TORCH syndromes

A number of disorders mimic TORCH infections on imaging. However, specific pseudo-TORCH syndromes (Type 1 and Type 2) have been defined and these are very rare diseases that share clinical and neuroimaging features of TORCH infections but have negative tests for TORCH pathogens. These children present with a variable degree of microcephaly, seizures, developmental delay and intracranial calcification [69–71].

Pseudo-TORCH syndrome-1

Pseudo-TORCH syndrome-1 (OMIM #251290) is a severe autosomal-recessive disorder caused by mutations in the *OCLN* gene encoding occludin (a tight-junction protein) [72]. Symptoms usually occur perinatally, with seizures, feeding abnormalities, microcephaly, quadriplegia and bulbar palsy [72]. Neuroimaging findings include a rudimentary pattern of brain development, typically with an hour-glass appearance

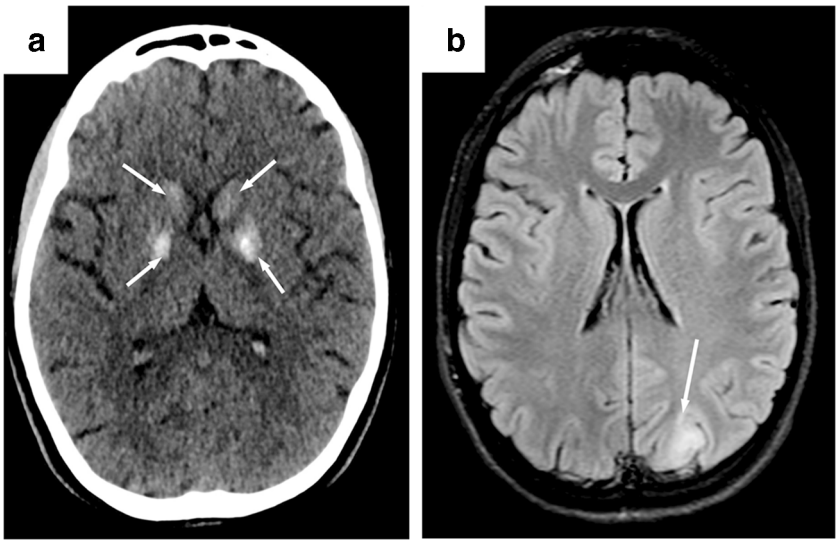

Fig. 6 Mitochondrial myopathy, encephalopathy, lactic acidosis, and stroke-like episodes (MELAS) in an 11-year-old girl with new stroke-like symptoms. **a** Axial nonenhanced CT image shows bilateral calcification in the basal ganglia (*arrows*). **b** Axial fluid-attenuated inversion recovery (FLAIR) MR image shows cortical hyperintensity in the left occipital lobe (*arrow*)

of the hemispheres and abnormal gyration (dysgyria). The cerebellum, brainstem and corpus callosum are typically hypoplastic. White matter volume is markedly reduced, with abnormally increased T2 signal and arrested myelination. Calcification in these children is arranged along with cortical bands but is also seen in the thalamus, cerebellum and pons (Fig. 9) [3].

Pseudo-TORCH syndrome-2

Pseudo-TORCH syndrome-2 (OMIM #617397) is an autosomal-recessive multisystem disorder caused by mutations in the *USP18* gene resulting in abnormal activation of the interferon immunologic pathway [69, 70]. Clinically, these children present with microcephaly, liver dysfunction, thrombocytopenia, early life respiratory failure, seizures and early infancy demise [73]. Postmortem examinations have demonstrated hemorrhage, ventriculomegaly, abnormal gyration of the temporal and parietal lobes, pachygyria, polymicrogyria, gray matter heterotopia, cerebellar hypoplasia and cortical destruction. Calcification in these children is periventricular and subcortical [70, 74]. Homozygous mutations in another tight-junction protein encoded by the *JAM3* gene can present a pseudo-TORCH phenotype, causing hemorrhagic destruction of the brain and congenital cataracts. Calcification in these children is characteristically subependymal [73].

Leukodystrophies associated with intracranial calcifications

Aicardi–Goutières syndrome

Aicardi–Goutières syndrome is a genetically heterogeneous group of encephalopathies characterized by a variable degree of cerebral atrophy, leukodystrophy and

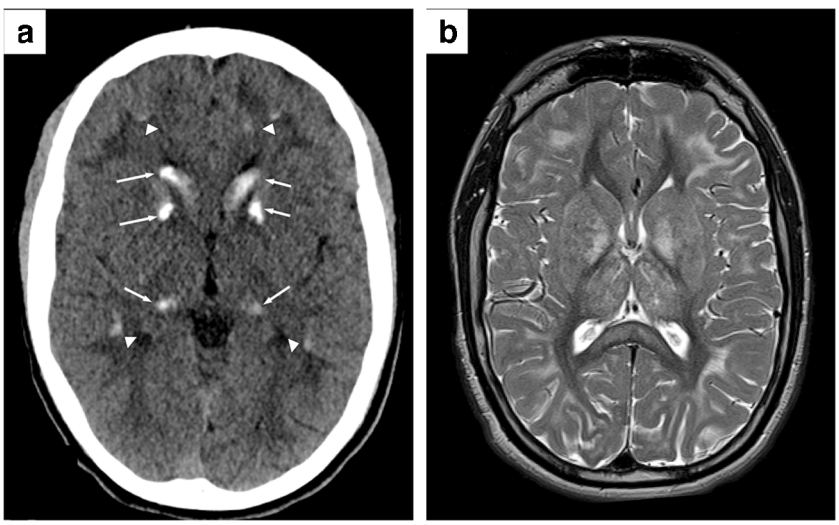

Fig. 7 Kearns–Sayre syndrome in a 14-year-old boy. **a** Axial nonenhanced CT image shows symmetrical calcification in the bilateral basal ganglia and thalami (*arrows*), bilateral scattered subcortical white matter calcifications (*arrowheads*), and diffuse bilateral symmetrical decreased density of the cerebral white matter. **b** Axial T2-weighted MR image shows diffuse T2 hyperintensity in the bilateral external capsules, globus pallidus, internal capsules, subcortical cerebral white matter and thalami, and in the corpus callosum

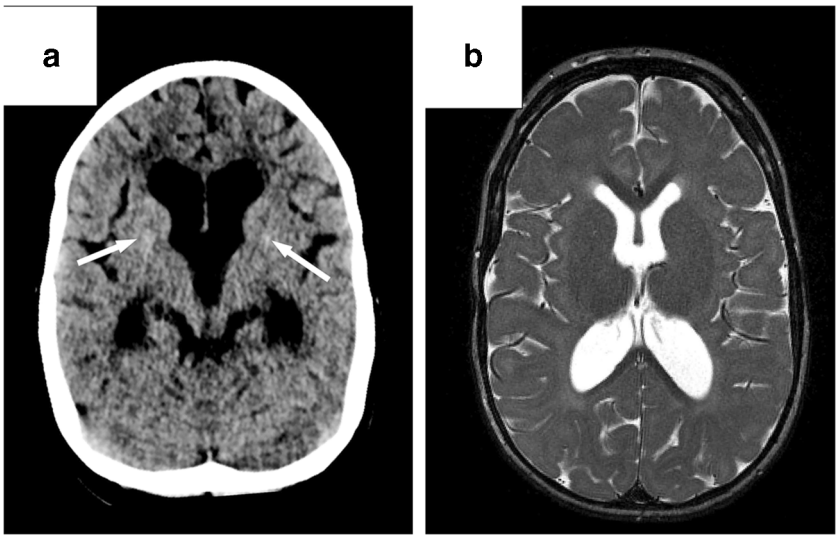

Fig. 8 Cockayne syndrome in a 6-year-old boy. **a**, **b** Axial nonenhanced CT (**a**) and axial T2-weighted MR (**b**) images show diffuse dilatation of the lateral and 3rd ventricles, generalized decrease in the white matter volume, and delayed myelination. Note the faint bilateral foci of calcification in the globi pallidi (*arrows* in **a**)

intracranial calcifications and as such, it is sometimes confused with TORCH disorders. These children might demonstrate chronic CSF lymphocytosis and increased CSF alpha-interferon and they have negative serology for TORCH pathogens [75]. Severe neurologic dysfunction becomes clinically apparent in infancy, manifesting as progressive microcephaly, spasticity, dystonic posturing and profound psychomotor delay and often death in

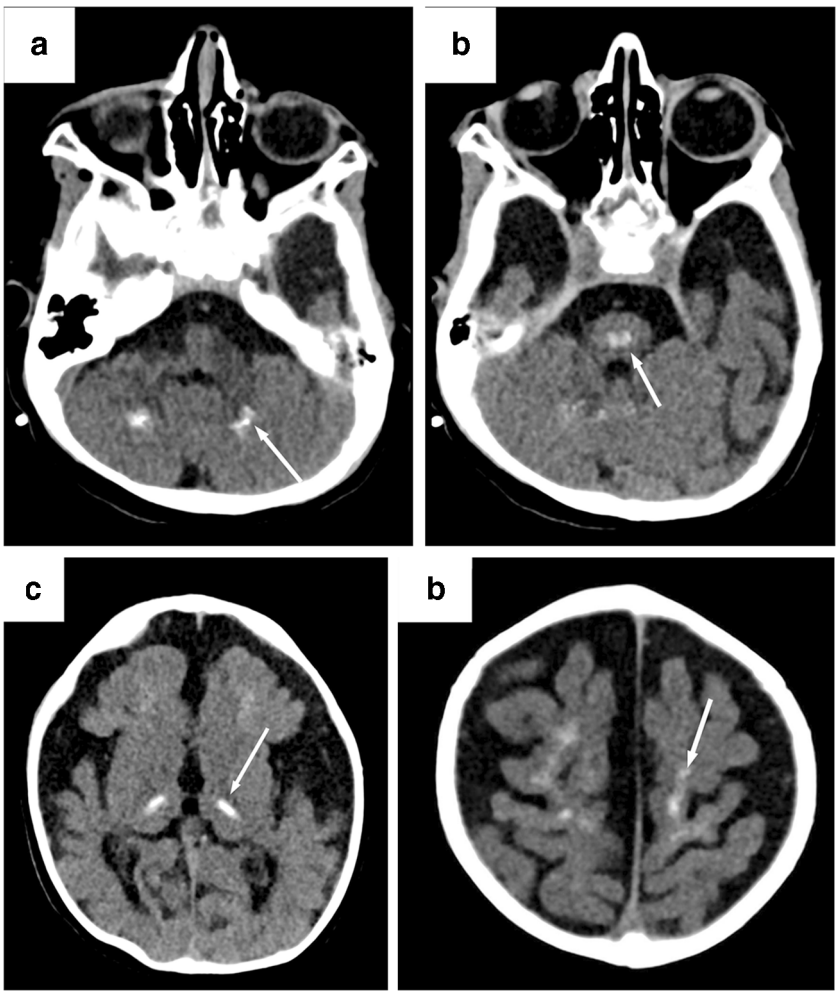

Fig. 9 Pseudo-TORCH syndrome-1 in a 5-month-old boy with global hypotonia, epilepsy, facial asymmetry, and decreased upper and lower extremity movement from *OCLN* mutation. **a**–**d** Axial nonenhanced CT images show diffuse enlargement of the extraaxial spaces, most prominent anteriorly, and bilateral frontal lobe volume loss associated with bilateral Sylvian fissures widening. Parenchymal calcification is noted in the (**a**) dentate nuclei, (**b**) central pons, (**c**) thalami and (**d**) in the frontal lobes (*arrows*). *TORCH* (toxoplasmosis, other [syphilis, varicella-zoster, parvovirus B19], rubella, cytomegalovirus and herpes) infection

childhood. Neuroimaging typically includes a variable degree of frontotemporal white matter rarefaction, cysts outside the frontotemporal regions, variable intracranial calcification (which can be severe and progressive) and delayed myelination [76]. Intracranial calcification is more commonly seen in the basal ganglia, cerebral white matter, thalamus, cerebellar hemispheres, dentate nucleus, brainstem and thalami (Fig. 10) [76, 77]. Children with *RNASET2* (ribonuclease T2) mutations (OMIM #612951) might present with overlapping clinical and radiologic features of cytomegalovirus (CMV) and Aicardi–Goutières syndrome. *RNASET2* is also known to cause cystic leukoencephalopathy without megalencephaly. There could be bilateral anterior temporal subcortical cysts and multifocal lobar white matter lesions with sparing of central white matter structures (Fig. 11) [78].

Krabbe disease

Globoid cell leukodystrophy (OMIM #245200), or Krabbe disease, is an autosomal-recessive lysosomal disease that affects the white matter of both central and peripheral nervous systems [79]. Krabbe disease is caused by a mutation of the *GALC* gene, leading to a deficiency in the lysosomal enzyme galactocerebroside beta-galactosidase, which regulates galactolipids' metabolism. The vast majority of these patients present in early infancy with extreme irritability, spasticity and developmental delay, leading to death

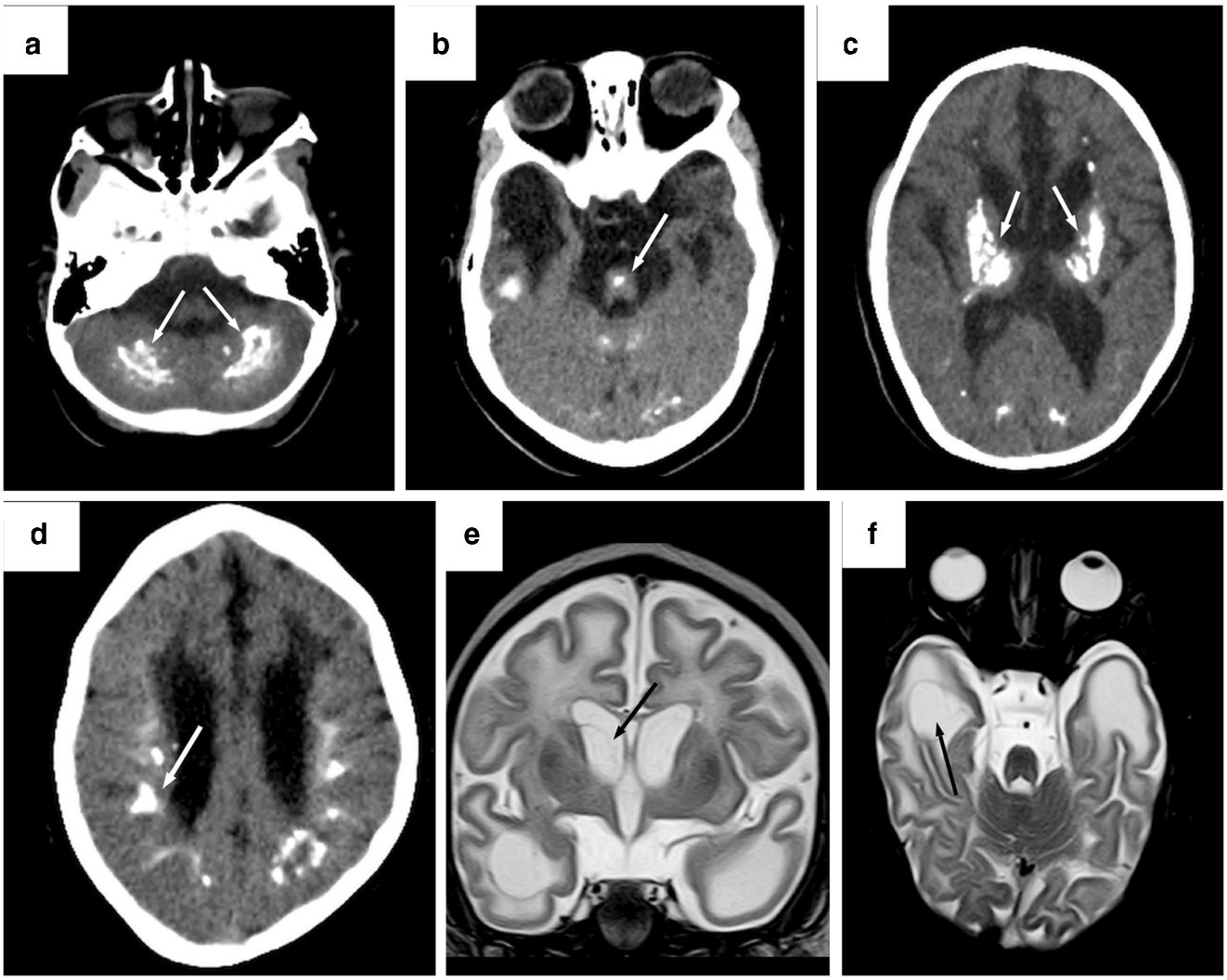

Fig. 10 Aicardi–Goutières syndrome in a 7-year-old boy with supra- and infratentorial calcification and diffuse white matter changes. **a**–**d** Axial nonenhanced CT images show calcification in the bilateral cerebellum in (**a**) (*arrows*); focal calcification in the deep pons, which is markedly atrophic in (**b**) (*arrow*); extensive and coarse calcification in the bilateral thalami and basal ganglia in (**c**) (*arrows*); and extensive and coarse calcification in the bilateral subcortical white matter in (**d**) (*arrow*). **e**, **f** T2-weighted MRI. Coronal image (**e**) shows extensive diffuse white matter T2 hyperintensity and a faint subependymal cyst (*arrow*), and axial image (**f**) shows a temporal lobe cyst on the right side (*arrow*)

before age 2 years [80]. Clinically, children might present with psychomotor regression, rigidity, peripheral neuropathy and increased CSF proteins. Neuroimaging reveals progressive cerebral atrophy and diffuse white matter abnormalities. CT might depict subtle bilateral thalamic and posterior periventricular hyperdensity, which likely corresponds to the accumulation of globoid cells with galactosylceramide buildup and calcium deposits (Fig. 12) [81].

Familial idiopathic basal ganglia calcification

Familial idiopathic basal ganglia calcification is a genetically heterogeneous entity composed of several conditions. Familial Idiopathic basal ganglia calcification-1 (IBGC1), caused by a heterozygous mutation in the *SLC20A2* gene and formerly known as Fahr disease, is a rare cause of intracranial calcification and is infrequently seen in childhood [82, 83]. IBGC1 is characterized by bilateral basal ganglia calcification-1 is characterized by bilateral basal ganglia calcification, accompanied by extrapyramidal and psychiatric symptoms. Children might also present with dystonia, poor balance and bradykinesia, seizures, developmental delay and progressive psychiatric symptoms such as aggressiveness and impulsivity [82]. Diagnosis is based on neuroimaging and normal levels of calcium, phosphate alkaline phosphatase and parathyroid hormone. Intracranial calcification in IBGC1 is typically extensive and coarse, more commonly in the basal ganglia (globus pallidus, putamen and caudate) (Fig. 13) and progresses with age with worsening of symptoms [82]. Other locations for intracranial calcification include the thalami, hippocampi, cerebral cortex, subcortical cerebral and cerebellar white matter and dentate nucleus [83].

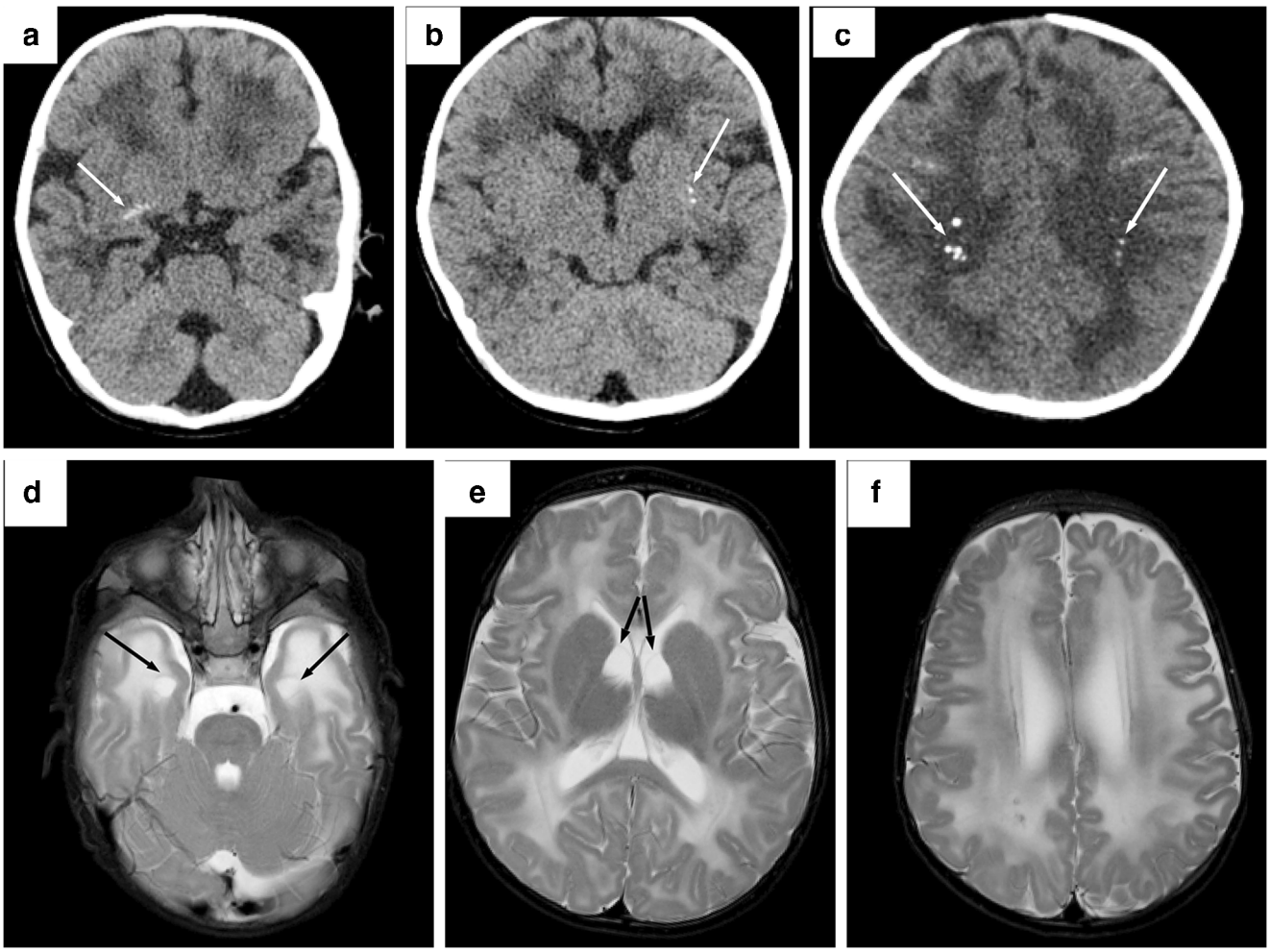

Fig. 11 *RNASET2* with global developmental delay in a 5-month-old boy. **a**, **b** Axial nonenhanced CT images show right (**a**) and left (**b**) basal ganglia calcification (*arrows*). **c** Axial nonenhanced CT image shows bilateral deep white matter calcification (*arrows*). **d**–**f** Axial T2-weighted MR images show extensive periventricular deep and subcortical supratentorial white matter hyperintensity. Note bilateral anteromedial temporal subcortical/subependymal cysts (*arrows* in **d**), bilateral subependymal cysts along lateral ventricles (*arrows* in **e**), and diffuse white matter signal abnormalities in (**f**)

Vascular causes of intracranial calcification

Intracranial calcification is a common finding in children with vascular malformations (Table 2) [84–92], namely arteriovenous malformations (Fig. 14), arteriovenous fistulas, developmental venous anomalies and cavernous malformations (Fig. 15). Calcium deposition might be secondary to chronic ischemia from vascular steal phenomenon, long-standing cortical venous reflux or chronic venous congestion. Similarly, specific arteriovenous shunting disorders such as vein of Galen malformations might also occasionally demonstrate calcifications. Other causes of intracranial calcification related to vascular diseases include atherosclerosis, healed hematomas and infarcts and in disorders of the microvasculature, such as *COL4A1*- and *COL4A2*-related disease (OMIM #175780 and OMIM # 614483, respectively) [9, 93].

Cortical laminar necrosis is a type of cortical infarction. Causes of cortical laminar necrosis include depletion of oxygen or glucose in anoxia, hypoglycemia, status epilepticus, ischemic stroke and less commonly in immunosuppressive therapy and chemoradiation [94–96]. On CT, cortical laminar necrosis presents as a gyriform linear hyperdensity in the superficial cortex, most frequently in the medial occipital lobes, but it can occur anywhere. Acute cortical laminar necrosis might present with edema and only rarely with hemorrhage and calcification. Calcification and hemorrhage are not typical in the acute phase but might be variably present later [97]. On MRI, cortical laminar necrosis typically demonstrates T1 hyperintensity because of the reactive tissue change of glia and deposition of fat-laden macrophages, typically not caused by hemorrhage. Enhancement might be present later between a week and a few months [98].

Neoplastic causes of intracranial calcifications

Calcifications are possible in many pediatric brain tumor groups and subtypes, with diverse frequency, size, number and imaging appearance, depending on the type of tumor. Important neuroimaging and clinical features that aid in the differential diagnosis of pediatric brain tumors are the age of presentation, tumor location, signal abnormalities on diffusion-weighted imaging, number of lesions and signs of brain invasion/dissemination at presentation [99]. The presence of calcification might be an adjunct finding that helps in the differentiation of brain masses along with other imaging features. Table 3 displays features of pediatric brain tumors that are more commonly associated with calcification [100–124], although this is not meant to be an exhaustive list because other tumor types rarely show calcification as well. A brief description of these tumor groups follows.

Craniopharyngiomas (World Health Organization [WHO] Grade I) are common suprasellar and occasionally intrasellar tumors that arise from remnants of the craniopharyngeal duct (Rathke pouch) [125], with a bimodal age distribution (5–14 years and 50–74 years) [126] (Fig. 16). Most of these tumors show cystic change and calcification [100, 101]. The differentiation between cystic and solid/cystic suprasellar lesions in children can be challenging. Because most pediatric craniopharyngiomas are known to have a high prevalence of calcification, its presence is often helpful to distinguish these from suprasellar gliomas or Rathke cleft cyst.

Subependymal giant cell astrocytomas (WHO Grade I) are benign, slow-growing intraventricular tumors typically near the foramen of Monro (unilateral or bilateral) in the context of tuberous sclerosis [104, 127] (Fig. 14 in Part 1 of this series). Calcifications are sometimes seen in subependymal

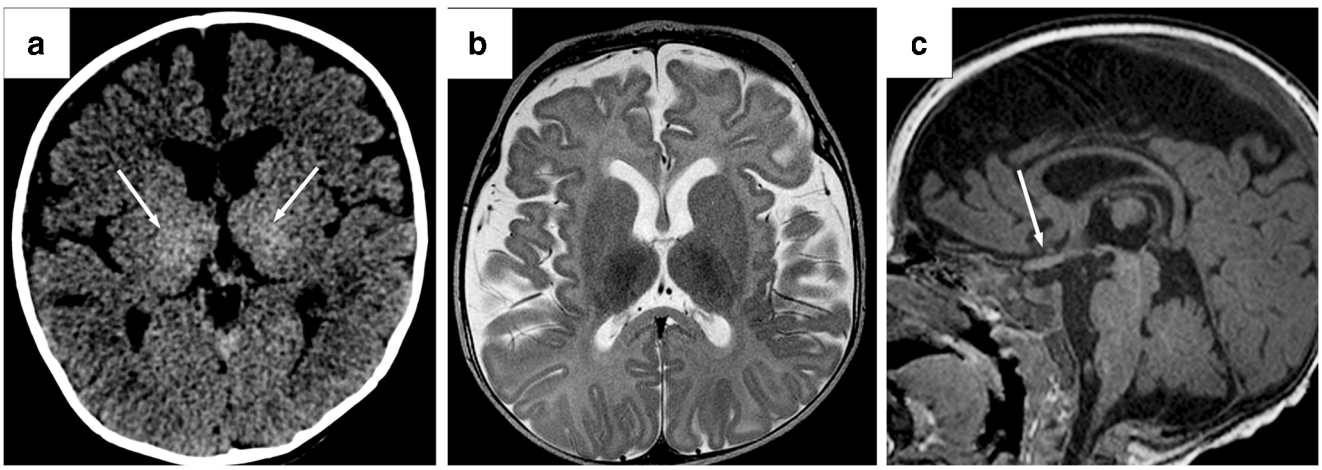

Fig. 12 Krabbe disease in a 2-year-old girl with developmental delay, dystonia and epilepsy. **a** Nonenhanced CT axial image shows subtle bilaterally increased density in the bilateral thalami (*arrows*). **b** Axial T2-weighted MR image shows mild prominence of the cerebrospinal fluid spaces, more so along bilateral frontal and temporal regions, mild enlargement of the lateral ventricles and symmetrical abnormal hyperintensity in the bilateral frontal and periatrial white matter, greater than expected for the age. **c** Sagittal T1-weighted MR image shows diffuse enlargement of the prechiasmatic intracranial segments of the optic nerves (*arrow*)

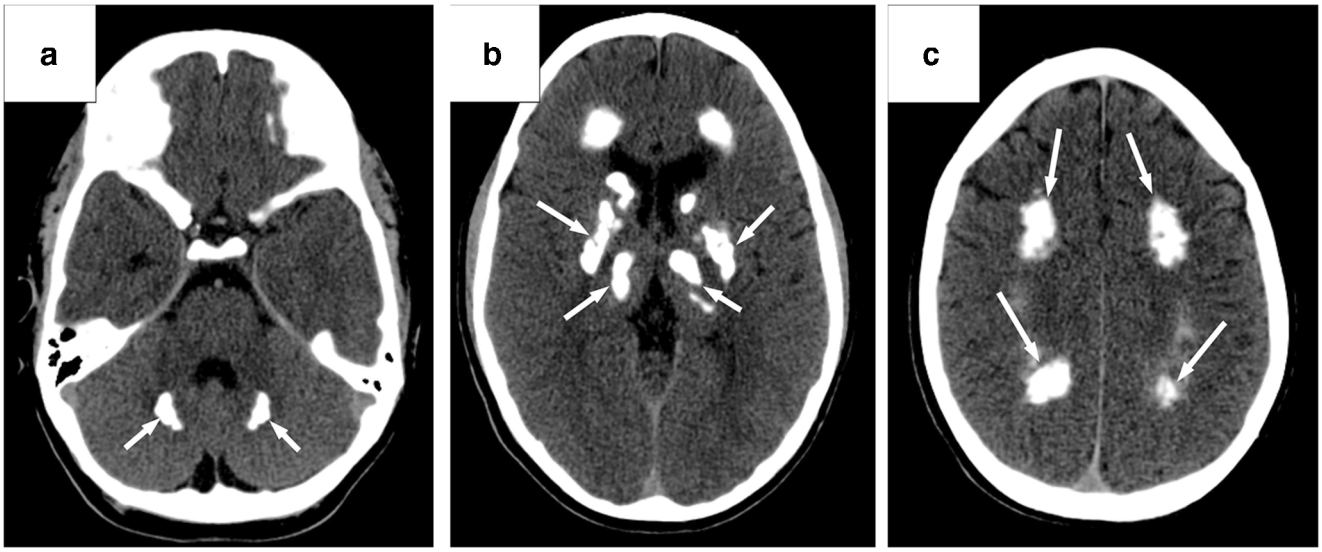

Fig. 13 Idiopathic basal ganglia calcification-1 (Fahr disease) in a 15-year-old boy with coarse infra- and supratentorial calcification. **a**–**c** Nonenhanced CT axial images show coarse bilateral calcification in the dentate nuclei (*arrows* in **a**), extensive bilateral basal ganglia and thalamic calcification (*arrows* in **b**), and chunky calcification in the bilateral deep white matter (*arrows* in **c**)

giant cell astrocytoma, although this could be caused by engulfment of nearby calcified subependymal nodules by the tumor.

Ependymomas (WHO Grade II/III) are more commonly located in the posterior fossa (4th ventricle) [128], often extending through the foramina of Luschka or Magendie (Fig. 17) [129]. Among posterior fossa tumors, ependymomas calcify most frequently compared to other tumors, although other tumors also calcify. Ependymomas uncommonly occur supratentorially, particularly in young children and are often associated with cysts and extensive calcification.

Gangliogliomas (WHO Grade I) are mixed glioneuronal tumors with neoplastic ganglion (neuronal) and glial components, typically cortically based, most commonly found in the temporal lobes and considered the most common neoplastic cause of refractory epilepsy in children and young adults [130] (Fig. 18). Calcifications, cysts and enhancing nodules are common features of these tumors, although they are not universally seen.

Medulloblastomas (WHO Grade IV) are the most common malignant pediatric central nervous system neoplasms (typically located in the posterior fossa) (Fig. 19) [111]. They show punctate calcifications with a lower frequency than ependymomas and typically have restricted diffusion.

Dysembryoplastic neuroepithelial tumors (WHO Grade I) are benign glioneuronal tumors typically associated with

Table 2 Vascular malformations associated with intracranial calcifications

Arteriovenous malformation (AVM)	Arteriovenous fistula	Developmental venous anomaly (DVA)	Cavernous malformation
– Tangle of dysplastic vessels forming a nidus fed by arteries and drained by veins without intervening capillaries [84, 85] – CT/MR angiography and conventional catheter angiography are useful neuroimaging modalities to demonstrate the arterial supply to the AVM, the nidus location and the venous drainage [86] – Punctate or curvilinear calcifications may be present	– Direct connections between arteries and veins without an intervening capillary web or nidus [86, 87] – Curvilinear calcifications in the subcortical white matter from chronic venous congestion or arterial steal phenomenon might be present [87]	– Typically asymptomatic variants of the normal transcerebral venous system [88] – Contrast-enhanced CT and MRI typically show enhancement of dilated veins with a "caput medusae" appearance without the presence of enlarged feeding arteries, but with the presence of a venous collector that drains to either the deep or superficial venous system – Stenosis of a DVA with subsequent chronic venous ischemia rarely results in dystrophic calcifications within the drained parenchymal territory [89]	– A frequent brain vascular malformation, forming clusters of blood-filled abnormal capillaries with varying degrees of thrombosis, occult in conventional angiograms [90, 91] – Isolated (sporadic) or multiple (familial) – Grouped into four categories, with Type II showing the classic popcorn appearance characterized by loculated areas of hemorrhage with hemosiderin deposits and surrounding gliosis [90] – May contain amorphous/punctate calcifications that can be seen on CT or MRI [92]

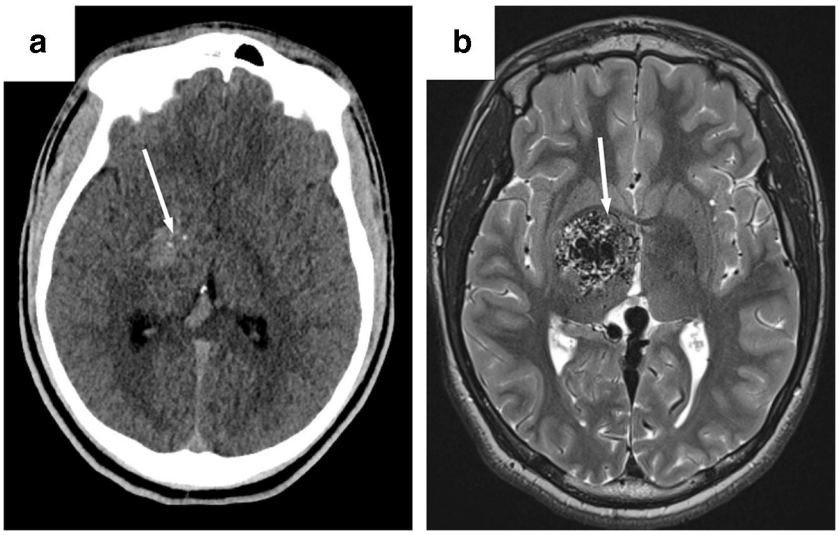

Fig. 14 Right thalamic/basal ganglia arteriovenous malformation in a 15-year-old boy with subacute left hemiparesis. **a** Nonenhanced CT axial image shows serpiginous hyperattenuating ill-defined mass with small foci of calcification (*arrow*). **b** Axial T2-weighted MR image shows serpiginous small and large vessels with mild mass effect (*arrow*)

intractable seizures in children/young adults (Fig. 20). They are most commonly supratentorial, predominantly cortical and characterized by a multinodular "bubbly" architecture and often a tail coursing toward the ventricles [131]. Calcification is much less common than in gangliogliomas and is usually punctate.

Choroid plexus tumors are uncommon intraventricular neoplasms derived from the choroid plexus epithelium (2–4% of intracranial tumors in children) [132]. They are sometimes present in choroid plexus papillomas (Fig. 21), typically located in the lateral ventricles (WHO Grade I/II), with children presenting with symptoms of increased intracranial pressure from increased CSF secretion such as headache, gait disturbances, papilledema, bulging fontanelle, macrocephaly and abducens nerve palsy. Calcifications are seen in about 25% of cases [133, 134]. Choroid plexus carcinomas (Fig. 22) are malignant tumors (WHO Grade III) typically located in the lateral ventricles and affecting young children (80% of cases), with a worse prognosis, particularly in cases of metastasis at the time of presentation. There is some imaging overlap among choroid plexus papillomas and choroid plexus carcinomas. Choroid plexus carcinoma enhancement is more heterogeneous because of necrosis, cysts and hemorrhage within the tumor, often with brain invasion. Calcification is found in 10–25% of these tumors [135].

Pilocytic astrocytomas are slow-growing (WHO Grade I) gliomas that typically occur in children and young adults and are seen anywhere along the central nervous system [132, 136] (cerebellum, optic nerves, optic chiasm, hypothalamus, brainstem, thalamus, basal ganglia, cerebral hemispheres and spinal cord), but most commonly in the cerebellum and suprasellar region (Fig. 23) [137, 138]. Calcification is uncommon in untreated posterior fossa and suprasellar pilocytic astrocytoma but is occasionally seen in other locations and after treatment.

Other intraaxial brain tumors also demonstrate calcification. Many superficial and cortical based brain tumors demonstrate calcification, the most common ones being ganglioglioma and dysembryoplastic neuroepithelial tumor, noted previously. Oligodendrogliomas are quite rare in

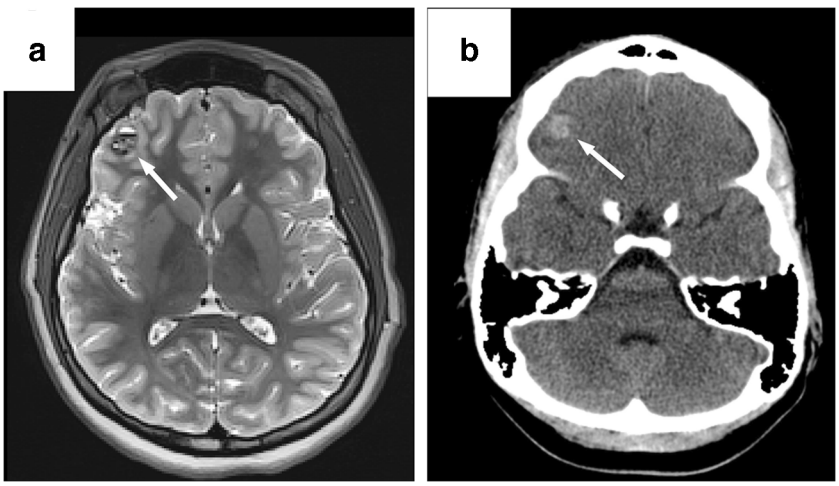

Fig. 15 Frontal lobe cavernous malformation in a 13-year-old girl with a new onset of seizures. **a** Axial T2-weighted MR image shows a small circumscribed and heterogeneous subcortical lesion in the right frontal lobe with the typical popcorn appearance for a cavernous malformation (*arrow*). **b** Nonenhanced CT axial image shows a small right frontal hyperdense partially calcified nodular lesion (*arrow*)

Table 3 Pediatric brain tumors more commonly associated with calcifications

Craniopharyngioma	SEGA	Ependymoma	Ganglioglioma	Medulloblastoma	DNET	Choroid plexus tumor	Pilocytic astrocytoma
– Typically, Gd^{+}, T1 hyper, cystic changes, and Ca^{+2} – Ca^{+2} is a prevalent and diagnostically important imaging finding in craniopharyngiomas with varying incidence [100, 101] – Ca^{+2} is more common in children (90%) than in adults (70%) [102]	– Most common brain tumor in TSC [103] –Found in 10–15% of TSC patients [103] – Probably arising from SENs (hamartomas) in the ventricular wall of TSC patients [103, 104] – CT: typically iso- to slightly hyperdense – MRI: T1 hypo- and T2 iso- to hyperintense – Often Gd^{+} – Ca^{+2} in 70% of cases, although may be caused by engulfment of nearby SEN by tumors [105]	– ↑ T2 signal due to myxoid material and cyst – ↓ T2 signal due to Ca^{+2} or blood [105] – Heterogeneous Gd+ – Ca^{+2} ~50% of cases [105, 106] – Variable Ca^{+2} (small/punctate, large/coarse) [107, 108] – Supratentorial ependymomas have coarse calcifications and cysts	– Partially cystic, with Gd^{+} mural nodule (40% of cases) – Nodule (T1 iso- to hypo- and T2 iso- to hyperintense) – Adjacent inner table scalloping can occur – Ca^{+2} in 28–41%, commonly large – Typically no mass effect or edema – Edema (rare) → Suspect a different diagnosis or anaplasia [109, 110]	– ↑ CT density – T1, T2 heterogeneity (cysts, blood, Ca^{+2}) [110, 111] – ↑ DWI, ↓ADC – Variable Gd^{+} – Cysts/necrosis in 50–90% of cases [112] – Ca^{+2} in 10–40% (small/speckled) [112] – Less commonly, Ca^{+2} (gross and extensive) [113–115] – DM Ca^{+2} in young patients suggests BCNS [116] – Ca^{+2} may also occur following RT in ~28% of cases (<3 years of age) [117]	– Well-defined (typically) – Peripheral masses, with a cyst-like appearance – Lacking mass effect or perilesional edema – May remodel the adjacent inner table of the skull – Hyperintense ring sign on FLAIR may occur [118] – Cystic in 24% of cases – Focal Gd^{+} in 20% – Ca^{+2} ~15% of cases [119]	Papillomas – Lobulated (cauliflower-like) – ↑ CT density with avid enhancement – T1 iso- to hypointense – T2 hyperintense, with intense Gd^{+} – Hydrocephalus – May show small flow voids → increased vascularity – Ca^{+2} in 25% of the cases (fin and speckled) Carcinomas – CT: ↑ density – MRI: T1 iso- to hypointense. T2 iso- to hypointense – Necrotic areas – Hydrocephalus, less common than in CPPs – Ca^{+2} ~20–25% of cases – At presentation, may show CSF seeding (neuroimaging of the entire neural axis recommended before surgery)	– T1 hypo- to isointense – T2 hyperintense – Cystic components (T1/T2 iso to CSF) – Solid components (variable signal) [120] – Variable Gd^{+} (none to avid) [120, 121] – Ca^{+2} (rare), flecks in the optic nerves, hypothalamus, thalamus or superficial tumors [122] – Extensive Ca^{+2} rarely occurs [123, 124]

ADC apparent diffusion coefficient map, *BCNS* basal cell nevus syndrome, Ca^{+2} calcification, *CPP* choroid plexus papilloma, *CSF* cerebrospinal fluid, *CT* computed tomography, *DM* dura mater, *DNET* dysembryoplastic neuroepithelial tumor, *DWI* diffusion-weighted imaging, *FLAIR* fluid-attenuated inversion recovery, Gd^{+} contrast enhancement, *MRI* magnetic resonance imaging, *RT* radiotherapy, *SEGA* subependymal giant cell astrocytoma, *SEN* subependymal nodule, *T1* T1-weighted imaging, *T2* T2-weighted imaging, *TSC* tuberous sclerosis complex

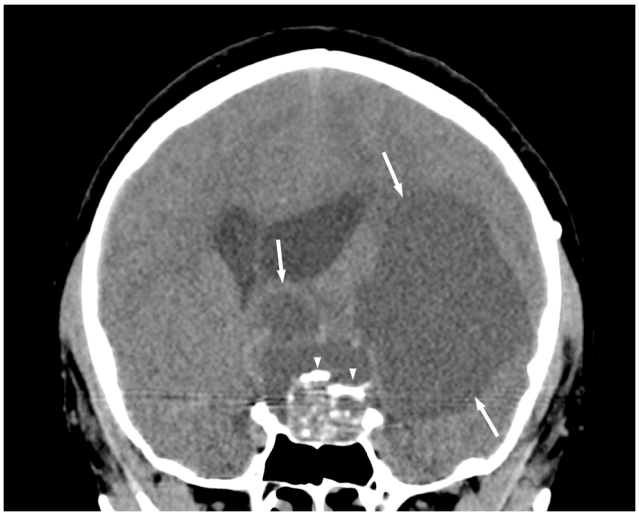

Fig. 16 Suprasellar solid/predominantly cystic craniopharyngioma in a 12-year-old boy with headaches and blurred vision. Nonenhanced CT coronal image shows the large suprasellar lobulated hypoattenuating cystic component of the mass (*arrows*) extending superiorly, compressing the 3rd ventricle and causing hydrocephalus, and laterally to the left frontal and temporal regions with mass effect. Note the solid heterogeneous mass in the sellar/suprasellar region with coarse calcification (*arrowheads*)

children, but they are often cortically based infiltrative masses with foci of dense, ribbon-like or chunky calcification [139]. Other uncommon hemispheric tumors such as desmoplastic infantile ganglioglioma might demonstrate calcification, but others such as pleomorphic astrocytomas or glioblastomas rarely calcify in children.

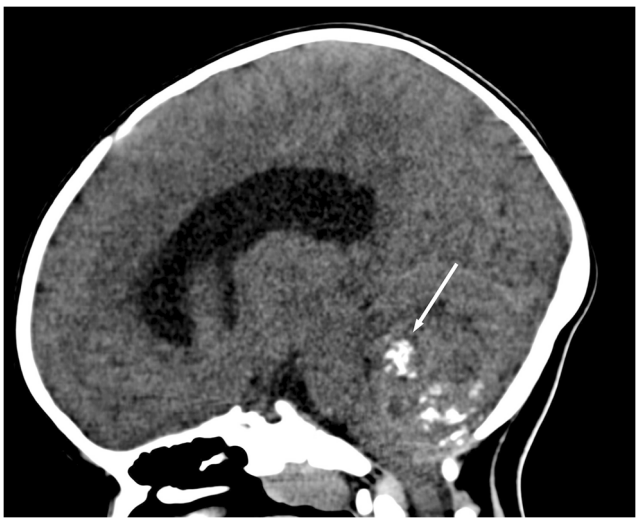

Fig. 17 Intraventricular posterior fossa ependymoma in an 8-year-old boy with headache, blurry vision and papilledema. The lesion was causing obstruction of the 4th ventricle with enlargement of the supratentorial ventricular system. Nonenhanced CT sagittal image shows a large and heterogeneous mass centered in the 4th ventricle with extension to the foramen of Magendie, with punctate and nodular scattered foci of calcification within the mass (*arrow*)

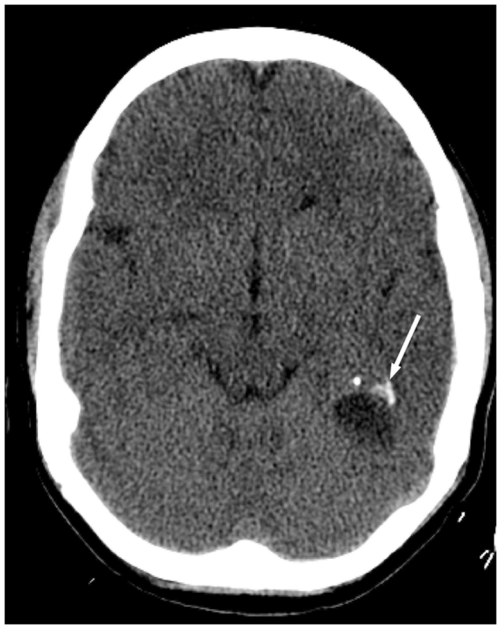

Fig. 18 Ganglioglioma. Nonenhanced CT axial image in an 11-year-old girl with intractable temporal lobe seizures caused by a ganglioglioma shows a mass lesion in the left posterior temporal lobe with low density and foci of calcification (*arrow*)

The pineal gland often calcifies as children get older. An intrinsic embryonal tumor such as pineoblastoma might have peripherally displaced "exploded" or "blasted" calcification. On the other hand, pineal germ cell tumors such as germinomas can engulf the pineal calcification [140]. These

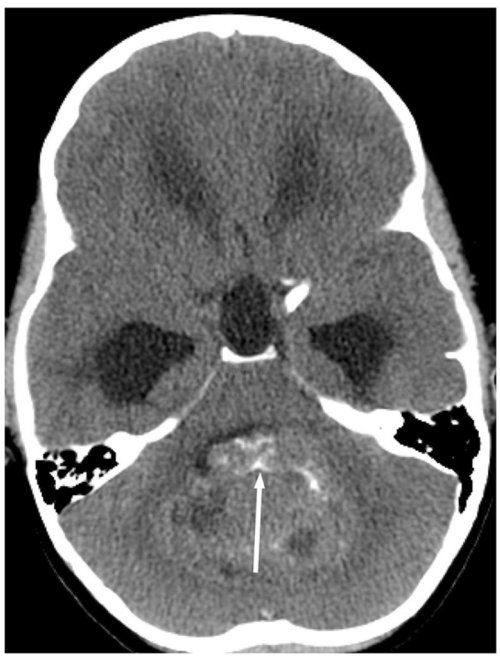

Fig. 19 Medulloblastoma in a 5-year-old boy with an unsteady gait, headaches, nausea, vomiting and hydrocephalus. Nonenhanced CT axial image shows a heterogeneous mixed cystic and solid mass with multiple small calcification foci projecting into the 4th ventricle (*arrow*)

Fig. 20 Dysembryoplastic neuroepithelial tumor (DNET) in a 4-year-old boy with temporal lobe epilepsy. Nonenhanced CT axial image shows a hypodense and partially calcified mass in the anteromedial left temporal lobe involving the white matter and the overlying cortex with no significant mass effect or edema (*arrow*)

features could help to differentiate these tumors, although they are not present in every case.

Intracranial extraaxial tumors might also demonstrate calcification. Meningiomas are rare in children but sometimes show calcifications, dural tail and bony changes. In addition, optic nerve sheath meningiomas, such as in children with neurofibromatosis Type 2, might have a tram-

Fig. 21 Choroid plexus papilloma in a 5-year-old boy. Nonenhanced CT axial image shows a fairly large lobulated dense mass in the atria of the left lateral ventricle associated with punctate calcification foci (*arrow*) and moderate hydrocephalus (*arrowhead*)

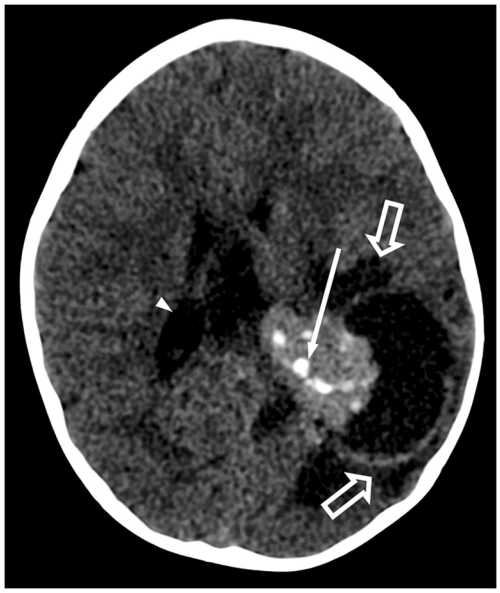

Fig. 22 Choroid plexus carcinoma in a 2-year-old girl. Nonenhanced CT axial image shows a fairly large and dense mass in the atria of the left lateral ventricle with punctate and coarse calcification (*thin arrow*), ventricular entrapment and mild hydrocephalus (*arrowhead*). In addition, note the vasogenic edema in the left parietal region with parenchymal invasion (*thick arrows*)

track appearance of calcification [141, 142]. Intracranial dermoids might show calcifications, particularly in their capsule [143]. Teratomas, which are typically seen in neonates as congenital tumors or in the pineal region, sometimes demonstrate calcifications along with other features such as fat and solid soft-tissue components. Some tumors originating from the skull base protrude intracranially and

Fig. 23 Pilocytic astrocytoma in a 7-year-old boy. Nonenhanced CT axial image shows a large supratentorial mass involving the hypothalamus, medial temporal lobe, inferior basal ganglia and midbrain on the right with peripheral calcification (*arrow*)

are commonly associated with calcifications. These include entities such as chordomas (typically in the midline central and posterior skull base) and chondrosarcomas (more frequently off midline such as from the petro-occipital synchondrosis), although chondrosarcomas of the skull base are rare in children.

Post-treatment changes after brain tumor chemoradiation therapy might also result in calcification. The calcification could be within the residual tumor tissue or in the brain parenchyma outside the tumor itself. Post-treatment mineralizing microangiopathy, which is characterized by calcium deposition in small vessels from fibrinoid necrosis following radiation and chemotherapy, occurs more commonly in children than in adults [144]. On neuroimaging, mineralizing microangiopathy might be seen as T2 signal abnormalities and multiple small calcifications in the basal ganglia, white matter and cortex [145].

Miscellaneous causes of intracranial calcification

Intracranial calcification is also found in cases of intracranial lipomas, either within the lesion, in its capsule or in the adjacent cerebral tissue [146]. These intracranial lipomas might be midline and associated with dysgenesis of the corpus callosum. Alternatively, lipomas might be seen in the quadrigeminal or suprasellar cisterns. Intracranial calcification can also be seen secondary to carbon monoxide poisoning [147]. Intracranial calcifications can also be secondary to cranial surgeries (after burr holes and device insertions, such as shunt catheters), some of which might be tiny bone chips introduced intracranially subsequent to skull drilling. Occasionally, calcifications are seen around long-standing indwelling shunt catheters [148]. Calcifications of the petroclinoid ligament at the skull base can be seen in children and sometimes mimic internal carotid artery calcification at its lacerum segment. The presence of an os suprapetrosum of Meckel, an incidental small focus of ossification in the same vicinity, can also be confused with carotid calcification [149].

Misoprostol is a synthetic prostaglandin E1 analog used to treat and prevent gastroduodenal injury following nonsteroidal anti-inflammatory drug use. Off-label indications include abortion/labor induction, management of miscarriage, uterine cervix ripening preparation before surgical procedures and postpartum hemorrhage [150]. Misoprostol has well-known teratogenic effects, mainly if used in the first months of pregnancy. There is a strong association between attempted abortions with misoprostol and Möbius syndrome [151], which might manifest with congenital palsy of multiple cranial nerves, particularly the 6th and 7th [152]. People with Möbius syndrome might present with brainstem hypoplasia, deformity of the rostral brainstem, absence of the hypoglossal prominence (hypoglossal nuclei hypoplasia) and cerebellar hypoplasia [152, 153]. Calcifications, when present, occur typically in the rostral pons and medulla, involving the nuclei of the 4th, 6th, 7th or 12th cranial nerves (Fig. 24) [151].

Fig. 24 Misoprostol use. Axial nonenhanced CT image in a 3-month-old boy shows bilateral punctate calcification (*arrowheads*) in the dorsal pons, involving the bilateral abducens nuclei secondary to maternal use of misoprostol

Bilateral symmetrical horn- or almond-shape calcifications affecting the amygdala and basal ganglia are typical in cases of lipoid proteinosis (Urbach–Wiethe disease) [154, 155]. Calcifying pseudoneoplasms of the neuraxis are rare fibro-osseous lesions that can display large well-defined calcifications and are very rarely seen during childhood [156].

Conclusion

A large variety of disorders in many categories demonstrate intracranial calcifications. Age, location of calcification and association with other neuroimaging findings are useful to arrive at the diagnosis. Narrowing the differential diagnosis can nevertheless be challenging in some conditions. In disorders that demonstrate intracranial calcification and typically are without additional imaging findings, such as congenital human immunodeficiency virus (HIV), Down syndrome, familial idiopathic basal ganglia calcification and parathyroid and thyroid dysfunction abnormalities, correlation with relevant clinical and laboratory findings is helpful to reach a more specific diagnosis. Several pediatric neurologic conditions such as central nervous system infections (TORCH

infections), phakomatosis, certain primary mitochondrial diseases and leukodystrophies, pseudo-TORCH syndromes, vascular malformations and neoplastic processes, on the other hand, are causes of intracranial calcification associated with various ancillary imaging findings reviewed in detail in this two-part article.

Compliance with ethical standards

Conflicts of interest None

References

1. Baba Y, Broderick DF, Uitti RJ et al (2005) Heredofamilial brain calcinosis syndrome. Mayo Clin Proc 80:641–651
2. Coomans C, Sieben A, Lammens M et al (2018) Early-onset dementia, leukoencephalopathy and brain calcifications: a clinical, imaging and pathological comparison of ALSP and PLOSL/Nasu Hakola disease. Acta Neurol Belg 118:607–615
3. Livingston JH, Stivaros S, Warren D, Crow YJ (2014) Intracranial calcification in childhood: a review of aetiologies and recognizable phenotypes. Dev Med Child Neurol 56:612–626
4. Pahuja L, Patras E, Sureshbabu S et al (2017) Labrune syndrome: a unique leukoencephalopathy. Ann Indian Acad Neurol 20:59–61
5. Labrune P, Lacroix C, Goutières F et al (1996) Extensive brain calcifications, leukodystrophy and formation of parenchymal cysts: a new progressive disorder due to diffuse cerebral microangiopathy. Neurology 46:1297–1301
6. Polvi A, Linnankivi T, Kivelä T et al (2012) Mutations in CTC1, encoding the CTS telomere maintenance complex component 1, cause cerebroretinal microangiopathy with calcifications and cysts. Am J Hum Genet 90:540–549
7. Simon AJ, Lev A, Zhang Y et al (2016) Mutations in STN1 cause Coats plus syndrome and are associated with genomic and telomere defects. J Exp Med 213:1429–1440
8. van der Knaap MS, Smit LME, Barkhof F et al (2006) Neonatal porencephaly and adult stroke related to mutations in collagen IV A1. Ann Neurol 59:504–511
9. Verbeek E, Meuwissen MEC, Verheijen FW et al (2012) COL4A2 mutation associated with familial porencephaly and small-vessel disease. Eur J Hum Genet 20:844–851
10. Revesz T, Fletcher S, al-Gazali LI, DeBuse P (1992) Bilateral retinopathy, aplastic anaemia and central nervous system abnormalities: a new syndrome? J Med Genet 29:673–675
11. Gowda VK, Vegda H, Benakappa N, Benakappa A (2018) Dihydropteridine reductase deficiency: a treatable neurotransmitter movement disorder masquerading as a refactory epilepsy due to novel mutation. Indian J Pediatr 85:812–813
12. Tesson C, Nawara M, Salih MAM et al (2012) Alteration of fatty-acid-metabolizing enzymes affects mitochondrial form and function in hereditary spastic parapledia. Am J Hum Genet 91:1051–1064
13. Barkhof F, Verrips A, Wesseling P et al (2000) Cerebrotendinous xanthomatosis: the spectrum of imaging findings and the correlation with neuropathologic findings. Radiology 217:869–876
14. Tumminelli G, Di Donato I, Guida V et al (2016) Oculodentodigital dysplasia with massive brain calcification and a new mutation of GJA1 gene. J Alzheimers Dis 49:27–30
15. Loddenkemper T, Grote K, Evers S et al (2002) Neurological manifestations of the oculodentodigital dysplasia syndrome. J Neurol 249:584–595
16. Hassed S, Li S, Mulvihill J et al (2017) Adams-Oliver syndrome review of the literature: refining the diagnostic phenotype. Am J Med Genet A 173:790–800
17. Al-Mane K, Al-Dayel F, McDonald P (1998) Intracranial calcification in Raine syndrome: radiological pathological correlation. Pediatr Radiol 28:820–823
18. AlBarrak ZM, Alqarni AS, Chalisserry EP, Anil S (2016) Papillon-Lefèvre syndrome: a series of five cases among siblings. J Med Case Rep 10:260
19. Utsumi T, Okada S, Izawa K et al (2017) A case with spondyloenchondrodysplasia treated with growth hormone. Front Endocrinol 8:157
20. Zaki MS, Selim L, El-Bassyouni HT et al (2016) Molybdenum cofactor and isolated sulphite oxidase deficiencies: clinical and molecular spectrum among Egyptian patients. Eur J Paediatr Neurol 20:714–722
21. Bosley TM, Alorainy IA, Oystreck DT et al (2014) Neurologic injury in isolated sulfite oxidase deficiency. Can J Neurol Sci 41: 42–48
22. Baishya J, Kesav P, Nampoothiri S et al (2018) Extensive extrapulvinar calcification in Fabry disease. Ann Indian Acad Neurol 21:309–310
23. Moore DF, Ye F, Schiffmann R, Butman JA (2003) Increased signal intensity in the pulvinar on T1-weighted images: a pathognomonic MR imaging sign of Fabry disease. AJNR Am J Neuroradiol 24:1096–1101
24. Lea ME, Harbord M, Sage MR (1995) Bilateral occipital calcification associated with celiac disease, folate deficiency and epilepsy. AJNR Am J Neuroradiol 16:1498–1500
25. Rajab A, Aldinger KA, El-Shirbini HA et al (2009) Recessive developmental delay, small stature, microcephaly and brain calcifications with locus on chromosome 2. Am J Med Genet A 149A: 129–137
26. Nicolas G, Sanchez-Contreras M, Ramos EM et al (2017) Brain calcifications and PCDH12 variants. Neurol Genet 3:e166
27. Cumming WA, Ohlsson A (1985) Intracranial calcification in children with osteopetrosis caused by carbonic anhydrase II deficiency. Radiology 157:325–327
28. Bosley TM, Salih MA, Alorainy IA et al (2011) The neurology of carbonic anhydrase Type II deficiency syndrome. Brain 134:3502–3515
29. Guo L, Bertola DR, Takanohashi A et al (2019) Bi-allelic CSF1R mutations cause skeletal dysplasia of dysosteosclerosis-Pyle disease spectrum and degenerative encephalopathy with brain malformation. Am J Hum Genet 104:925–935
30. Kawashima H, Kawano M, Masaki A, Sato T (1988) Three cases of untreated classical PKU: a report on cataracts and brain calcification. Am J Med Genet 29:89–93
31. Bosemani T, Felling RJ, Wyse E et al (2014) Neuroimaging findings in children with Keutel syndrome. Pediatr Radiol 44:73–78
32. Battisti C, Dotti MT, Cerase A et al (2002) The Primrose syndrome with progressive neurological involvement and cerebral calcification. J Neurol 249:1466–1468
33. Cleaver R, Berg J, Craft E et al (2019) Refining the Primrose syndrome phenotype: a study of five patients with ZBTB20 de novo variants and a review of the literature. Am J Med Genet A 179:344–349
34. Han C, Alkhater R, Froukh T et al (2016) Epileptic encephalopathy caused by mutations in the guanine nucleotide exchange factor DENND5A. Am J Hum Genet 99:1359–1367
35. Schulz PE, Weiner SP, Belmont JW, Fishman MA (1988) Basal ganglia calcifications in a case of biotinidase deficiency. Neurology 38:1326–1328
36. Ahmad I, Mukhtar G, Iqbal J, Ali SW (2015) Hereditary folate malabsorption with extensive intracranial calcification. Indian Pediatr 52:67–68

37. Rock MJ, Prenen J, Funari VA et al (2008) Gain-of-function mutations in TRPV4 cause autosomal dominant brachyolmia. Nat Genet 40:999–1003
38. Griffith AJ, Sprunger LK, Sirko-Osadsa DA et al (1998) Marshall syndrome associated with a splicing defect at the COL11A1 locus. Am J Hum Genet 62:816–823
39. McDermott A, Jesus AA, Liu Y et al (2013) A case of proteasome-associated auto-inflammatory syndrome with compound heterozygous mutations. J Am Acad Dermatol 69:e29–e32
40. Black JO (2016) Xeroderma pigmentosum. Head Neck Pathol 10: 139–144
41. Isojima T, Doi K, Mitsui J et al (2014) A recurrent de novo FAM111A mutation causes Kenny-Caffey syndrome Type 2. J Bone Miner Res 29:992–998
42. Bertamino M, Severino M, Schiaffino MC et al (2015) New insights into central nervous system involvement in FOP: case report and review of the literature. Am J Med Genet A 167A:2817–2821
43. Severino M, Bertamino M, Tortora D et al (2016) Novel asymptomatic CNS findings in patients with ACVR1/ALK2 mutations causing fibrodysplasia ossificans progressiva. J Med Genet 53: 859–864
44. Kamal NM, Alghamdi HA, Halabi AA et al (2017) Idiopathic hypoparathyroidism with extensive intracranial calcification in children: first report from Saudi Arabia. Medicine 96:e6347
45. Chen L, Chen B, Leng W et al (2015) Identification of a novel de novo GATA3 mutation in a patient with HDR syndrome. J Int Med Res 43:718–724
46. Nesbit MA, Hannan FM, Howles SA et al (2013) Mutations affecting G-protein subunit α11 in hypercalcemia and hypocalcemia. N Engl J Med 368:2476–2486
47. Tenhola S, Voutilainen R, Reyes M et al (2016) Impaired growth and intracranial calcifications in autosomal dominant hypocalcemia caused by a GNA11 mutation. Eur J Endocrinol 175:211–218
48. Cacciagli P, Desvignes J-P, Girard N et al (2014) AP1S2 is mutated in X-linked Dandy-Walker malformation with intellectual disability, basal ganglia disease and seizures (Pettigrew syndrome). Eur J Hum Genet 22:363–368
49. Smith RS, Kenny CJ, Ganesh V et al (2018) Sodium channel SCN3A ($Na_v1.3$) regulation of human cerebral cortical folding and oral motor development. Neuron 99:905–913.e7
50. Roizen J, Levine MA (2012) Primary hyperparathyroidism in children and adolescents. J Chin Med Assoc 75:425–434
51. de la Plaza LR, Ramia Ángel JM, Arteaga Peralta V et al (2016) Brain calcifications and primary hyperparathyroidism. Cirugía Española 94:e5–e7
52. Bokhari SA, Khan PM, Bokhari EA (2016) Extensive intracranial calcification presenting with neurological symptoms due to primary hypoparathyroidism and secondary hyperparathyroidism: two case reports. J Health Spec 4:157–160
53. Markowitz ME, Underland L, Gensure R (2016) Parathyroid disorders. Pediatr Rev 37:524–535
54. Fulop M, Zeifer B (1991) Case report: extensive brain calcification in hypoparathyroidism. Am J Med Sci 302:292–295
55. Haft AS (1953) Idiopathic hypoparathyroidism and cataract; report of four cases. AMA Arch Ophthalmol 50:455–461
56. Mendelsohn DB, Hertzanu Y (1984) Hypoparathyroidism with cerebral calcification extending beyond the extrapyramidal system. A case report. S Afr Med J 65:781–782
57. Mantovani G (2011) Clinical review: pseudohypoparathyroidism: diagnosis and treatment. J Clin Endocrinol Metab 96:3020–3030
58. Visconti P, Posar A, Scaduto MC et al (2016) Neuropsychiatric phenotype in a child with pseudohypoparathyroidism. J Pediatr Neurosci 11:267–270
59. Hanley P, Lord K, Bauer AJ (2016) Thyroid disorders in children and adolescents: a review. JAMA Pediatr 170:1008–1019
60. Dinizio A, Vincent J, Nickerson J (2016) Intracranial calcifications in the pediatric age group: an imaging review. J Pediatr Neuroradiol 4:049–059
61. El-Hattab AW, Adesina AM, Jones J, Scaglia F (2015) MELAS syndrome: clinical manifestations, pathogenesis and treatment options. Mol Genet Metab 116:4–12
62. Malhotra K, Liebeskind DS (2016) Imaging of MELAS. Curr Pain Headache Rep 20:54
63. Kearns TP (1958) Retinitis pigmentosa, external ophthalmoplegia and complete heart block. AMA Arch Ophthalmol 60:280
64. Saneto RP, Friedman SD, Shaw DWW (2008) Neuroimaging of mitochondrial disease. Mitochondrion 8:396–413
65. Scheibye-Knudsen M, Croteau DL, Bohr VA (2013) Mitochondrial deficiency in Cockayne syndrome. Mech Ageing Dev 134:275–283
66. Wilson BT, Stark Z, Sutton RE et al (2016) The Cockayne syndrome natural history (CoSyNH) study: clinical findings in 102 individuals and recommendations for care. Genet Med 18:483–493
67. Sonmez FM, Celep F, Ugur SA, Tolun A (2006) Severe form of Cockayne syndrome with varying clinical presentation and no photosensitivity in a family. J Child Neurol 21:333–337
68. Koob M, Laugel V, Durand M et al (2010) Neuroimaging in Cockayne syndrome. AJNR Am J Neuroradiol 31:1623–1630
69. Patnaik A, Mishra SS, Das S (2017) Extensive intracranial calcification of pseudo-TORCH syndrome with features of Dandy-Walker malformation. Asian J Neurosurg 12:541–543
70. Knoblauch H, Tennstedt C, Brueck W et al (2003) Two brothers with findings resembling congenital intrauterine infection-like syndrome (pseudo-TORCH syndrome). Am J Med Genet A 120A: 261–265
71. Cohen MC, Karaman I, Squier W et al (2012) Recurrent pseudo-TORCH appearances of the brain presenting as "Dandy-Walker" malformation. Pediatr Dev Pathol 15:45–49
72. O'Driscoll MC, Daly SB, Urquhart JE et al (2010) Recessive mutations in the gene encoding the tight junction protein occludin cause band-like calcification with simplified gyration and polymicrogyria. Am J Hum Genet 87:354–364
73. Mochida GH, Ganesh VS, Felie JM et al (2010) A homozygous mutation in the tight-junction protein JAM3 causes hemorrhagic destruction of the brain, subependymal calcification and congenital cataracts. Am J Hum Genet 87:882–889
74. Meuwissen MEC, Schot R, Buta S et al (2016) Human USP18 deficiency underlies Type 1 interferonopathy leading to severe pseudo-TORCH syndrome. J Exp Med 213:1163–1174
75. Ali M, Highet LJ, Lacombe D et al (2006) A second locus for Aicardi-Goutieres syndrome at chromosome 13q14-21. J Med Genet 43:444–450
76. La Piana R, Uggetti C, Roncarolo F et al (2016) Neuroradiologic patterns and novel imaging findings in Aicardi-Goutières syndrome. Neurology 86:28–35
77. Uggetti C, La Piana R, Orcesi S et al (2009) Aicardi-Goutieres syndrome: neuroradiologic findings and follow-up. AJNR Am J Neuroradiol 30:1971–1976
78. Tonduti D, Orcesi S, Jenkinson EM et al (2016) Clinical, radiological and possible pathological overlap of cystic leukoencephalopathy without megalencephaly and Aicardi-Goutières syndrome. Eur J Paediatr Neurol 20:604–610
79. Graziano ACE, Cardile V (2015) History, genetic and recent advances on Krabbe disease. Gene 555:2–13
80. Farina L, Bizzi A, Finocchiaro G et al (2000) MR imaging and proton MR spectroscopy in adult Krabbe disease. AJNR Am J Neuroradiol 21:1478–1482
81. Percy AK, Odrezin GT, Knowles PD et al (1994) Globoid cell leukodystrophy: comparison of neuropathology with magnetic resonance imaging. Acta Neuropathol 88:26–32

82. Wang H, Shao B, Wang L, Ye Q (2015) Fahr's disease in two siblings in a family: a case report. Exp Ther Med 9:1931–1933
83. Wu Y (2012) Fahr's disease: pediatric presentation of a rare neurodegenerative disorder (P01.236). Neurology 78:P01.236–P01.236
84. Lawton MT, Rutledge WC, Kim H et al (2015) Brain arteriovenous malformations. Nat Rev Dis Primers 1:15008
85. Solomon RA, Connolly ES (2017) Arteriovenous malformations of the brain. N Engl J Med 376:1859–1866
86. Geibprasert S, Pongpech S, Jiarakongmun P et al (2010) Radiologic assessment of brain arteriovenous malformations: what clinicians need to know. Radiographics 30:483–501
87. Weon YC, Yoshida Y, Sachet M et al (2005) Supratentorial cerebral arteriovenous fistulas (AVFs) in children: review of 41 cases with 63 non choroidal single-hole AVFs. Acta Neurochir 147:17–31
88. Saito Y, Kobayashi N (1981) Cerebral venous angiomas: clinical evaluation and possible etiology. Radiology 139:87–94
89. Dehkharghani S, Dillon WP, Bryant SO, Fischbein NJ (2010) Unilateral calcification of the caudate and putamen: association with underlying developmental venous anomaly. AJNR Am J Neuroradiol 31:1848–1852
90. Raychaudhuri R, Batjer HH, Awad IA (2005) Intracranial cavernous angioma: a practical review of clinical and biological aspects. Surg Neurol 63:319–328
91. Zabramski JM, Wascher TM, Spetzler RF et al (1994) The natural history of familial cavernous malformations: results of an ongoing study. J Neurosurg 80:422–432
92. Wang KY, Idowu OR, Lin DDM (2017) Radiology and imaging for cavernous malformations. Handb Clin Neurol 143:249–266
93. Livingston J, Doherty D, Orcesi S et al (2011) COL4A1 mutations associated with a characteristic pattern of intracranial calcification. Neuropediatrics 42:227–233
94. Donaire A, Carreno M, Gómez B et al (2006) Cortical laminar necrosis related to prolonged focal status epilepticus. J Neurol Neurosurg Psychiatr 77:104–106
95. Sawada H, Udaka F, Seriu N et al (1990) MRI demonstration of cortical laminar necrosis and delayed white matter injury in anoxic encephalopathy. Neuroradiology 32:319–321
96. Khong P-L, Ng K-C, Kwong DLW et al (2005) Cortical laminar necrosis in childhood intracranial germ cell tumor survivors. Pediatr Blood Cancer 44:412–415
97. Niwa T, Aida N, Shishikura A et al (2008) Susceptibility-weighted imaging findings of cortical laminar necrosis in pediatric patients. AJNR Am J Neuroradiol 29:1795–1798
98. Samain JL, Haven E, Gille M, Mathys P (2011) Typical CT and MRI features of cortical laminar necrosis. JBR-BTR 94:357
99. Dang M, Phillips PC (2017) Pediatric brain tumors. Continuum 23:1727–1757
100. Mollá E, Martí-Bonmatí L, Revert A et al (2002) Craniopharyngiomas: identification of different semiological patterns with MRI. Eur Radiol 12:1829–1836
101. Zhao X, Yi X, Wang H, Zhao H (2012) An analysis of related factors of surgical results for patients with craniopharyngiomas. Clin Neurol Neurosurg 114:149–155
102. Lee IH, Zan E, Bell WR et al (2016) Craniopharyngiomas: radiological differentiation of two types. J Korean Neurosurg Soc 59:466–470
103. Jóźwiak S, Nabbout R, Curatolo P, participants of the TSC Consensus Meeting for SEGA and Epilepsy Management (2013) Management of subependymal giant cell astrocytoma (SEGA) associated with tuberous sclerosis complex (TSC): clinical recommendations. Eur J Paediatr Neurol 17:348–352
104. Kim J-Y, Jung T-Y, Lee K-H, Kim S-K (2017) Subependymal giant cell astrocytoma presenting with tumoral bleeding: a case report. Brain Tumor Res Treat 5:37–41
105. Yuh EL, Barkovich AJ, Gupta N (2009) Imaging of ependymomas: MRI and CT. Childs Nerv Syst 25:1203–1213
106. Mermuys K, Jeuris W, Vanhoenacker PK et al (2005) Best cases from the AFIP: supratentorial ependymoma. Radiographics 25:486–490
107. Morrison G, Sobel DF, Kelley WM, Norman D (1984) Intraventricular mass lesions. Radiology 153:435–442
108. Koeller KK, Sandberg GD, Armed Forces Institute of Pathology (2002) From the archives of the AFIP. Cerebral intraventricular neoplasms: radiologic-pathologic correlation. Radiographics 22:1473–1505
109. Castillo M, Davis PC, Takei Y, Hoffman JC (1990) Intracranial ganglioglioma: MR, CT and clinical findings in 18 patients. AJNR Am J Neuroradiol 11:109–114
110. Zentner J, Wolf HK, Ostertun B et al (1994) Gangliogliomas: clinical, radiological and histopathological findings in 51 patients. J Neurol Neurosurg Psychiatry 57:1497–1502
111. Packer RJ (1999) Childhood medulloblastoma: progress and future challenges. Brain and Development 21:75–81
112. Dangouloff-Ros V, Varlet P, Levy R et al (2018) Imaging features of medulloblastoma: conventional imaging, diffusion-weighted imaging, perfusion-weighted imaging and spectroscopy: from general features to subtypes and characteristics. Neurochirurgie https://doi.org/10.1016/j.neuchi.2017.10.003
113. Koeller KK, Rushing EJ (2003) From the archives of the AFIP: medulloblastoma: a comprehensive review with radiologic-pathologic correlation. Radiographics 23:1613–1637
114. Prasad A, Madan VS, Buxi TB, Prasad ML (1991) Medulloblastoma with extensive calcification. Neuroradiology 33:447–448
115. Nelson M, Diebler C, Forbes WS (1991) Paediatric medulloblastoma: atypical CT features at presentation in the SIOP II trial. Neuroradiology 33:140–142
116. Stavrou T, Dubovsky EC, Reaman GH et al (2000) Intracranial calcifications in childhood medulloblastoma: relation to nevoid basal cell carcinoma syndrome. AJNR Am J Neuroradiol 21:790–794
117. Davis PC, Hoffman JC, Pearl GS, Braun IF (1986) CT evaluation of effects of cranial radiation therapy in children. AJR Am J Roentgenol 147:587–592
118. Parmar HA, Hawkins C, Ozelame R et al (2007) Fluid-attenuated inversion recovery ring sign as a marker of dysembryoplastic neuroepithelial tumors. J Comput Assist Tomogr 31:348–353
119. Thom M, Toma A, An S et al (2011) One hundred and one dysembryoplastic neuroepithelial tumors: an adult epilepsy series with immunohistochemical, molecular genetic and clinical correlations and a review of the literature. J Neuropathol Exp Neurol 70:859–878
120. Arai K, Sato N, Aoki J et al (2006) MR signal of the solid portion of pilocytic astrocytoma on T2-weighted images: is it useful for differentiation from medulloblastoma? Neuroradiology 48:233–237
121. Chourmouzi D, Papadopoulou E, Konstantinidis M et al (2014) Manifestations of pilocytic astrocytoma: a pictorial review. Insights Imaging 5:387–402
122. Lee YY, Van Tassel P, Bruner JM et al (1989) Juvenile pilocytic astrocytomas: CT and MR characteristics. AJR Am J Roentgenol 152:1263–1270
123. Kim YE, Shin HJ, Suh Y-L (2012) Pilocytic astrocytoma with extensive psammomatous calcification in the lateral ventricle: a case report. Childs Nerv Syst 28:649–652
124. Aydemir F, Kardes O, Kayaselçuk F, Tufan K (2016) Massive calcified cerebellar pilocytic astrocytoma with rapid recurrence: a rare case. J Korean Neurosurg Soc 59:533–536
125. Prabhu VC, Brown HG (2005) The pathogenesis of craniopharyngiomas. Childs Nerv Syst 21:622–627

126. Bunin GR, Surawicz TS, Witman PA et al (1998) The descriptive epidemiology of craniopharyngioma. J Neurosurg 89:547–551
127. Tahiri Elousrouti L, Lamchahab M, Bougtoub N et al (2016) Subependymal giant cell astrocytoma (SEGA): a case report and review of the literature. J Med Case Rep 10:35
128. Nowak J, Seidel C, Pietsch T et al (2015) Systematic comparison of MRI findings in pediatric ependymoblastoma with ependymoma and CNS primitive neuroectodermal tumor not otherwise specified. Neuro Oncol 17:1157–1165
129. Plaza MJ, Borja MJ, Altman N, Saigal G (2013) Conventional and advanced MRI features of pediatric intracranial tumors: posterior fossa and suprasellar tumors. AJR Am J Roentgenol 200:1115–1124
130. Borja MJ, Plaza MJ, Altman N, Saigal G (2013) Conventional and advanced MRI features of pediatric intracranial tumors: supratentorial tumors. AJR Am J Roentgenol 200:W483–W503
131. Stanescu Cosson R, Varlet P, Beuvon F et al (2001) Dysembryoplastic neuroepithelial tumors: CT, MR findings and imaging follow-up: a study of 53 cases. J Neuroradiol 28:230–240
132. Louis DN, Ohgaki H, Wiestler OD et al (2007) The 2007 WHO classification of tumours of the central nervous system. Acta Neuropathol 114:97–109
133. Naeini RM, Yoo JH, Hunter JV (2009) Spectrum of choroid plexus lesions in children. AJR Am J Roentgenol 192:32–40
134. Safaee M, Oh MC, Bloch O et al (2013) Choroid plexus papillomas: advances in molecular biology and understanding of tumorigenesis. Neuro Oncol 15:255–267
135. Haroun RI, Li KW, Khan W et al (2000) Primary tumors of the choroid plexus. Contemp Neurosurg 22:1–8
136. Tibbetts KM, Emnett RJ, Gao F et al (2009) Histopathologic predictors of pilocytic astrocytoma event-free survival. Acta Neuropathol 117:657–665
137. Manik M, Rajesh S, Poonam S, Anchal G (2012) Densely calcified pilocytic astrocytoma in the sellar/suprasellar region. Int J Clin Pediatr 1:129–132
138. Burkhard C, Di Patre P-L, Schüler D et al (2003) A population-based study of the incidence and survival rates in patients with pilocytic astrocytoma. J Neurosurg 98:1170–1174
139. Creach KM, Rubin JB, Leonard JR et al (2012) Oligodendrogliomas in children. J Neurooncol 106:377–382
140. Smirniotopoulos JG, Rushing EJ, Mena H (1992) Pineal region masses: differential diagnosis. Radiographics 12:577–596
141. Mehta N, Bhagwati S, Parulekar G (2009) Meningiomas in children: a study of 18 cases. J Pediatr Neurosci 4:61–65
142. Deftereos SP, Karagiannakis GK, Spanoudaki A et al (2008) Optic nerve sheath meningioma: a case report. Cases J 1:423
143. D'Amore A, Borderi A, Chiaramonte R et al (2013) CT and MR studies of giant dermoid cyst associated to fat dissemination at the cortical and cisternal cerebral spaces. Case Rep Radiol 2013:239258
144. Pruzincová L, Steno J, Srbecký M et al (2009) MR imaging of late radiation therapy- and chemotherapy-induced injury: a pictorial essay. Eur Radiol 19:2716–2727
145. Mamlouk MD, Handwerker J, Ospina J, Hasso AN (2013) Neuroimaging findings of the post-treatment effects of radiation and chemotherapy of malignant primary glial neoplasms. Neuroradiol J 26:396–412
146. Durão C, Pedrosa F (2017) Undiagnosed intracranial lipoma associated with sudden death. Hum Pathol Case Reports 7:39–40
147. Illum F (1980) Calcification of the basal ganglia following carbon monoxide poisoning. Neuroradiology 19:213–214
148. Abbas M, Bakhaidar M, Baeesa SS (2018) Intracranial dystrophic calcification of ventriculoperitoneal shunt: a case report. Pediatr Neurosurg 53:356–359
149. Currarino G, Weinberg A (1974) Os supra petrosum of Meckel. AJR Am J Roentgenol Radium Ther Nucl Med 121:139–142
150. Allen R, O'Brien BM (2009) Uses of misoprostol in obstetrics and gynecology. Rev Obstet Gynecol 2:159–168
151. Guedes ZCF (2014) Möbius syndrome: misoprostol use and speech and language characteristics. Int Arch Otorhinolaryngol 18:239–243
152. Picciolini O, Porro M, Cattaneo E et al (2016) Moebius syndrome: clinical features, diagnosis, management and early intervention. Ital J Pediatr 42:56
153. Ouanounou S, Saigal G, Birchansky S (2005) Möbius syndrome. AJNR Am J Neuroradiol 26:430–432
154. Staut CC, Naidich TP (1998) Urbach-Wiethe disease (lipoid proteinosis). Pediatr Neurosurg 28:212–214
155. Gonçalves FG, de Melo MB, de L Matos V et al (2010) Amygdalae and striatum calcification in lipoid proteinosis. AJNR Am J Neuroradiol 31:88–90
156. García Duque S, Medina Lopez D, Ortiz de Méndivil A, Diamantopoulos Fernández J (2016) Calcifying pseudoneoplasms of the neuraxis: report on four cases and review of the literature. Clin Neurol Neurosurg 143:116–120